

## Development of a non-perennial to ephemeral fluvial system in continental fault-bounded basin – an example from the early Permian Krajanów Formation of the Intra-Sudetic Basin (NE Bohemian Massif)

Aleksander KOWALSKI<sup>1</sup>, \* and Magdalena FURCA<sup>1</sup>

<sup>1</sup> Polish Geological Institute – National Research Institute, Lower Silesia Branch, Al. Jaworowa 19, 50–122 Wrocław, Poland; ORCID: 0000-0003-4963-3995 [A.K.], 0009-0006-6328-2262 [M.F.]



Kowalski, A., Furca, M., 2023. Development of a non-perennial to ephemeral fluvial system in continental fault-bounded basin – an example from the early Permian Krajanów Formation of the Intra-Sudetic Basin (NE Bohemian Massif). *Geological Quarterly*, 67: 31, doi: 10.7306/gq.1701

Non-perennial to ephemeral fluvial systems dominated by seasonal discharge fluctuations and episodic rapid flood-flow events are typical of arid to semi-arid climatic conditions. Dryland fluvial systems have been described from many ancient and modern, predominantly tectonically-controlled sedimentary basins across the globe. This study provides detailed sedimentological analysis and palaeoenvironmental interpretation of the lowermost part of the early Permian (?Asselian) Krajanów Formation exposed within the continental, fault-bounded Intra-Sudetic Basin (ISB), located on the NE periphery of Bohemian Massif. High-resolution sedimentological logging and facies analysis indicate that the early Permian fluvial system in this area was dominated by ephemeral fluvial processes influenced strongly by a semi-arid to arid climate. Rapid (?catastrophic) flood events led to episodic sedimentation of vertically and laterally amalgamated fluvial channel infills, with abundant upper flow regime structures as well as poorly channelized, laterally extensive sheet-like bodies of sandstone. The overbank deposits are poorly preserved due to frequent lateral shifting of the channels. Soft-sediment deformation structures formed due to events of river bank collapse as well as debris flow facies point to high-energy, waning flows. It is concluded that deposition occurred on broad, terminal-type alluvial fans, probably in their proximal- to medial segments within a distributive fluvial system of the Permian Intra-Sudetic Basin. Petrographic composition and measured palaeocurrent directions show that the sediment was sourced from the neighbouring massifs – the Sowie Mts. Massif to the east, the Bardo Structure and a hypothetical Southern Massif to the south/south-east.

Key words: palaeoclimate, distributive fluvial system, endorheic basins, palaeogeographic reconstruction, Asselian, Sudetes.

### INTRODUCTION

Deposits of dryland ephemeral fluvial systems are well known both from modern (Williams, 1971; Picard and High, 1973; Foley, 1978; Stear, 1985; Tooth, 2000; Billi, 2011; Camarasa-Belmonte, 2016) and ancient sedimentary successions across the globe (Tunbridge, 1984; Olsen, 1987; Deluca and Eriksson, 1989; North and Taylor, 1996; Long, 2006; Lowe and Arnott, 2016; Priddy and Clarke, 2020). According to Tooth (2000), the general and descriptive term “dryland” refers to regions dominated by hyper-arid, arid, semi-arid or dry-subhumid climate conditions. In contrast to their perennial and semi-perennial counterparts, ephemeral fluvial systems developed under the influence of such climatic regimes are dominated by seasonal, highly variable discharge and episodic flash flood-flow events as a direct response to strongly seasonal precipitation (Picard and High, 1973; Stear, 1985; Lange, 2005; Shanafield et al., 2021). Flows in ephemeral rivers and streams

are relatively shallow and are characterized by high sediment concentrations. According to Reid and Frostick (1987), concentration of suspended sediment during flash floods in an ephemeral stream is from 35 to 1,700 times higher than in perennial ones. Thus, deposition of clastic material in dryland rivers is controlled by poorly-confined to unconfined, sheet-like Newtonian flows as well as episodic, non-Newtonian pseudo-plastic flows (including hyperconcentrated flows), both related to rapid, high-discharge seasonal flood events (Karcz, 1972; Lange, 2005). These processes resulted in elements of fluvial architecture which are in general dominated by upper flow regime bedforms (i.e. parallel lamination), isolated erosional scours, intraformational conglomerates and structures indicating subaerial exposure of sediment (i.e. mud cracks, raindrop imprints; e.g., Picard and High, 1973; Colombera et al., 2013).

Recent studies have shown that continental sedimentary basins, especially those developed in dryland settings, are dominated by distributive fluvial systems (DFSs; Weissmann et al., 2010; Owen et al., 2015). Morphologically, these aggradational systems are characterized by (i) convex-up, lobate (fan-shaped) topography (ii) radial pattern of river channels, (iii) downstream decrease in channel depth and also (iv) bifurcation of channels (Kelly and Olsen, 1993; Cain and Mountray, 2009;

\* Corresponding author: e-mail: [aleksander.kowalski@pgi.gov.pl](mailto:aleksander.kowalski@pgi.gov.pl)

Received: June 1, 2023; accepted: June 27, 2023; first published online: October 10, 2023

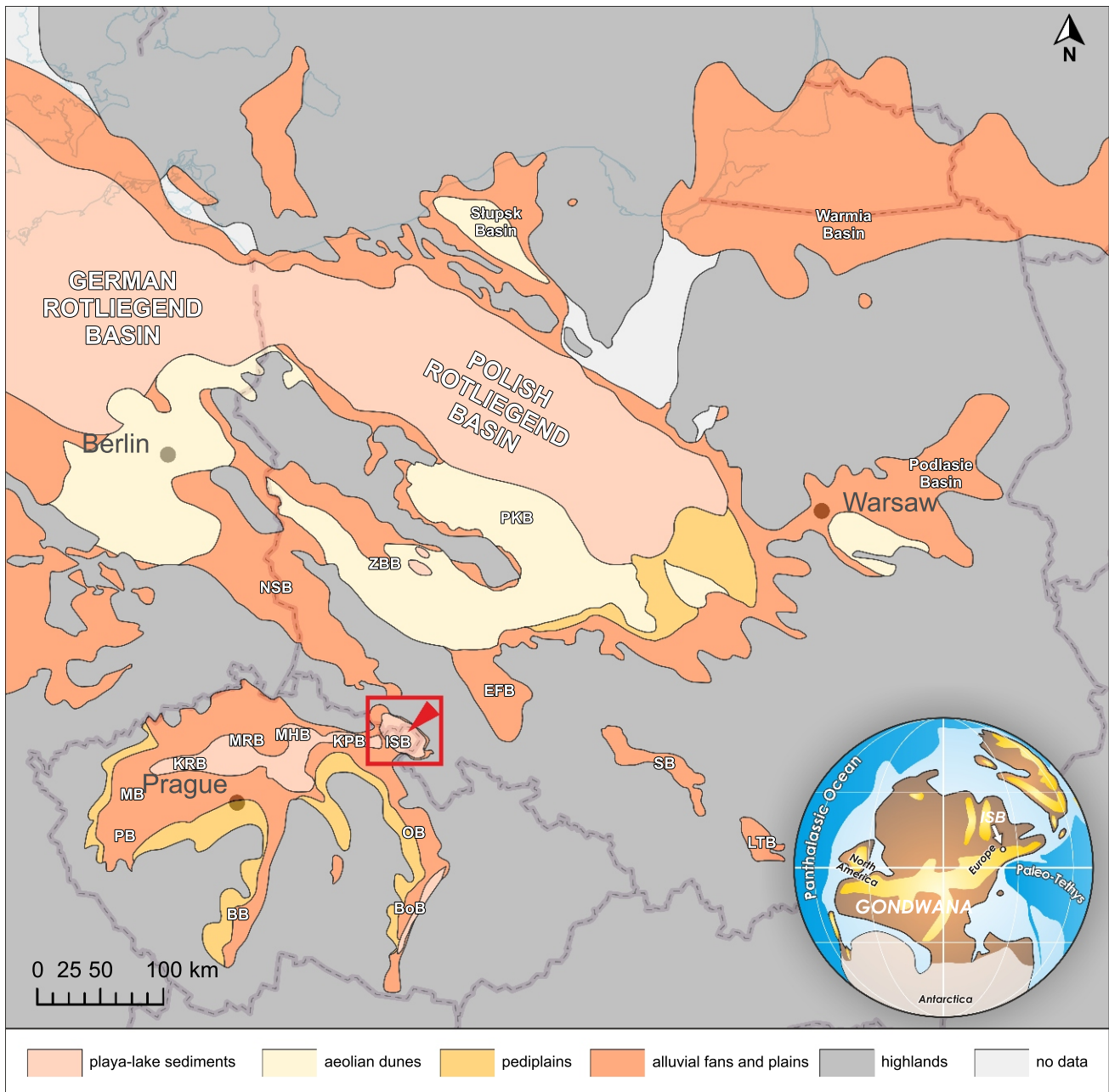


**Fig. 1. Generalized facies map and extent of the Lower Permian in the NE Bohemian Massif and Central Western Europe (modified after Holub, 1975; Opluštil and Pešek, 1998; Pokorski, 1998; Doornenbal and Stevenson, 2010; Kiersnowski, 2013; Kiersnowski and Peryt, 2023), Early Permian world after Scotese (2013)**

EFB – Eastern Fore-Sudetic Basin, LTB – Liplas-Tarnawa Basin, NSB – North Sudetic Basin, PKB – Pniewy-Książ Wlkp. Basin, SB – Sławków Basin, ZBB – Zielona Góra–Borzęcin Basin; basins within and around the Bohemian Massif: BB – Blanice Basin, BoB – Boskovice Basin with Mirosław occurrence in south, ISB – Intra-Sudetic Basin, KPB – Karkonosze Piedmont Basin, KRB – Kladno–Rakovník Basin, MB – Manětín Basin, MHB – Mnichovo Hradiště Basin, MRB – Mšeno–Roudnice Basin, OB – Orlice Basin, PB – Plzeň Basin

Weissmann et al., 2010). Such large-scale features of the fluvial system are an apparent result of dry climate and resultant water losses (also referred to in the literature as "transmission losses"), related to high rates of evapotranspiration and infiltration into the dry substrate/streambed (Lange, 2005; Shanfield et al., 2021). In general, the deposits of DFSs preserved in the rock record typically display gradual downstream decrease in channel-fill elements and downstream increase in fine-grained, sheetflood and floodplain deposits, respectively (Owen et al., 2015; Priddy and Clarke, 2021). These spatial, basin-scale trends are predominantly associated with downstream de-

crease in grain-size within a sedimentary succession. Additionally, deposits of fluvial origin may co-occur and interact with coeval aeolian strata (Glennie, 1970; Al-Masrahy and Mountney, 2015; Priddy and Clarke, 2021).

In general, semi-arid to dry-subhumid continental climatic conditions, characterized by a highly seasonal climate, were typical of the early Permian Polish Rotliegend Basin area (Kiersnowski, 1997; Karnkowski, 1999; Kiersnowski and Buniak, 2016), forming the easternmost part of the Southern Permian Basin (SPB) of Central Europe (Fig. 1). The Bohemian Massif constituted one of the source areas bounding this

depositional area to the south and south-west (Holub, 1972; Doornenbal and Stevenson, 2010). Within and around the Bohemian Massif, numerous fault-controlled extensional and transtensional basins developed during the terminal phases of the Variscan orogeny (Holub, 1975; Malkovský, 1987; Mastalerz, 1996; Opluštil and Pešek, 1998; Uličný et al., 2002; Wojewoda et al., 2016). The NW–SE-trending Intra-Sudetic Basin (ISB) constituted one of several such semi-enclosed, fault-bounded depressions. The Permian volcano-sedimentary succession of this basin shows a distinct, large-scale cyclic structure and comprises successive, fining-upwards continental megasequences (cf. Nemeč et al., 1982; Mastalerz et al., 1993; Awdankiewicz et al., 2003). This megacyclic structure is thought to have originated from tectonic activity and is attributed to relatively rapid, fault-controlled subsidence of the basin floor (Nemeč et al., 1982; Wojewoda and Mastalerz, 1989).

This study interprets the continental red-bed assemblage of the early Permian (?Asselian) deposits of the lowermost Krajanów Formation, which constitutes one of these fining-upwards megasequences. The Krajanów Formation is predominantly exposed within the easternmost, proximal region of the Intra-Sudetic Basin. The overarching objective of this paper is to improve understanding of the early Permian palaeogeography and depositional history of the Intra-Sudetic Basin based on integrated outcrop-scale sedimentological studies, palaeocurrent measurements, and facies- and architectural-element analysis. Additionally, the authors critically discuss the role of tectonic activity and contemporary climate change during deposition of the lowermost Krajanów Formation in the Intra-Sudetic Basin.

## GEOLOGICAL SETTING

The Krajanów Formation occupies the lowermost part of the early Permian (?Asselian) succession in the Polish part of the NW–SE-trending Intra-Sudetic Basin situated within the Sudetic Block, at the NE periphery of the Bohemian Massif (Fig. 2). The Intra-Sudetic Basin developed since the middle to early late Viséan, at ~333–335 Ma (Turnau et al., 2002), as a narrow intramontane trough and underwent complex evolution from the early Carboniferous to the Late Cretaceous (Augustyniak and Grocholski, 1968; Nemeč et al., 1982; Awdankiewicz et al., 2003). During the early Carboniferous (middle-early late Viséan?, cf. Turnau et al., 2002), the northern and western sectors of the trough were filled with coarse-grained clastic sediments, interpreted as piedmont-like, alluvial fan and braided-river deposits (Teisseyre, 1975; Dziedzic and Teisseyre, 1990). The resultant, lowermost part of the Carboniferous succession shows a large-scale cyclic structure and is subdivided into the Ciechanowice, Figlów, Nagórník, Stare Bogaczowice and Lubomin formations (Nemeč et al., 1982). During the late Viséan, the northern parts of the ISB were flooded by a relatively shallow sea (Żakowa, 1958). Along the northern margin of the Basin there developed a system of fan deltas and small-radius fans, which encroached into the marine embayment (Mastalerz, 1995). The upper Viséan-lower Serpukhovian (Górecka-Nowak et al., 2021) marine and deltaic deposits are distinguished in this part of the ISB as the Szczawno Formation. The overlying upper Carboniferous deposits, assigned to the Wałbrzych, Biały Kamień and Żacler formations, consist of predominantly fluvial, coal-bearing successions (Nemeč, 1984; Mastalerz, 1996; Kurowski, 1998). These successions are overlain by the Glinik Formation, which repre-

sents deposits of braided and meandering rivers (Ihnatowicz, 2005). The overlying, fining upwards cyclothem of the Ludwikowice Formation consists of typical red bed-type deposits accumulated in alluvial-fan, fluvial and lacustrine settings (Mastalerz et al., 1993; Wójcik-Tabol et al., 2021; Nowak et al., 2022).

During the early Permian the ISB constituted a semi-enclosed, southwestern outlier of the Polish Rotliegend Basin (Southern Permian Basin of Central Europe; Fig. 1). The Permian, non-marine sedimentary-volcanogenic succession of the ISB exhibits a distinct, large-scale cyclic structure and comprises three successive, fining-upwards continental megasequences up to 700 m-thick in total (Nemeč et al., 1982; Awdankiewicz et al., 2003). These megasequences include the lower Permian (Asselian–Sakmarian) deposits, which are traditionally distinguished as three formations: the Krajanów, Słupiec and Radków formations (Fig. 3). These formations are mainly composed of alluvial fan and fluvial deposits in their lower to middle parts, and fluvial/deltaic to lacustrine deposits in the uppermost parts (Nemeč et al., 1982; Wojewoda and Mastalerz, 1989). Such megacyclic structure of the Permian basin fill is thought to have originated from tectonic activity and is attributed to relatively rapid, fault-controlled episodic subsidence of the basin floor (Nemeč et al., 1982; Wojewoda and Mastalerz, 1989). The basin infilling was interrupted several times by late Carboniferous to early Permian, polymodal volcanic and subvolcanic activity as well as tectonic deformation (Awdankiewicz, 1999, 2022). The latter is reflected in several hiatuses in the sedimentary record. The main recognized breaks in deposition took place especially during the Gzhelian (Intra-Stephanian/Franconian tectonic event according to Opluštil et al., 2016) and during the Sakmarian (Saale tectonic event; Opluštil et al., 2016). The first hiatus is linked by some authors with the first stage of Intra-Sudetic Basin inversion (Żelaźniewicz et al., 2011). The Permian sedimentary succession of the ISB is discordantly overlain by clastic deposits assigned to the Lower Triassic (i.e. Buntsandstein). Early Triassic siliciclastic deposition in the Intra-Sudetic Basin was dominated by fluvial sedimentation within a gently sloping alluvial plain, drained by shallow, braided rivers towards the northwest and north (Mroczkowski and Mader, 1985; Kowalski, 2020). After a ~140 My break in sedimentation, the lower Triassic deposits were discordantly overlain by Upper Cretaceous marine strata which attain a thickness of up to 400 m in the Intra-Sudetic area (Wojewoda, 1997; Kowalski, 2021). The maximum stratigraphic thickness of the basin infill reaches ~11,000 m (Nemeč et al., 1982; Fig. 3).

The Intra-Sudetic Basin is currently interpreted as a large-scale inverted synclinal unit, ~70 km long and 35 km wide, and termed the Intra-Sudetic Synclinorium (Oberc, 1972; Żelaźniewicz and Aleksandrowski, 2008; Żelaźniewicz et al., 2011). This geological unit has a present-day areal extent of ~1800 km<sup>2</sup>. Its current tectonic structure is an apparent result of Late Cretaceous–early Paleogene and Neogene compressional tectonic events (Oberc, 1972; Żelaźniewicz et al., 2011; Głuszyński and Aleksandrowski, 2022). These events led to inversion and significant tectonic deformation of the basin infill which was dissected by mainly NW–SE and NE–SW-trending fault systems. It has been widely considered that some of these faults were active during infilling of the basin as well as controlling the intra-basinal magmatic activity during the Carboniferous-Permian (Augustyniak and Grocholski, 1968; Awdankiewicz, 2022).

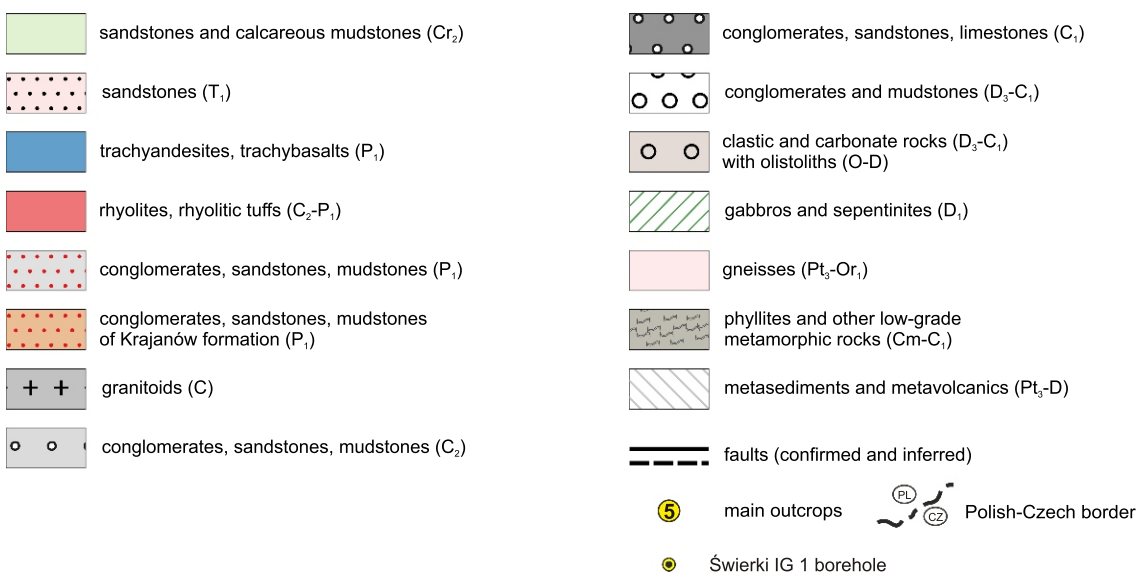
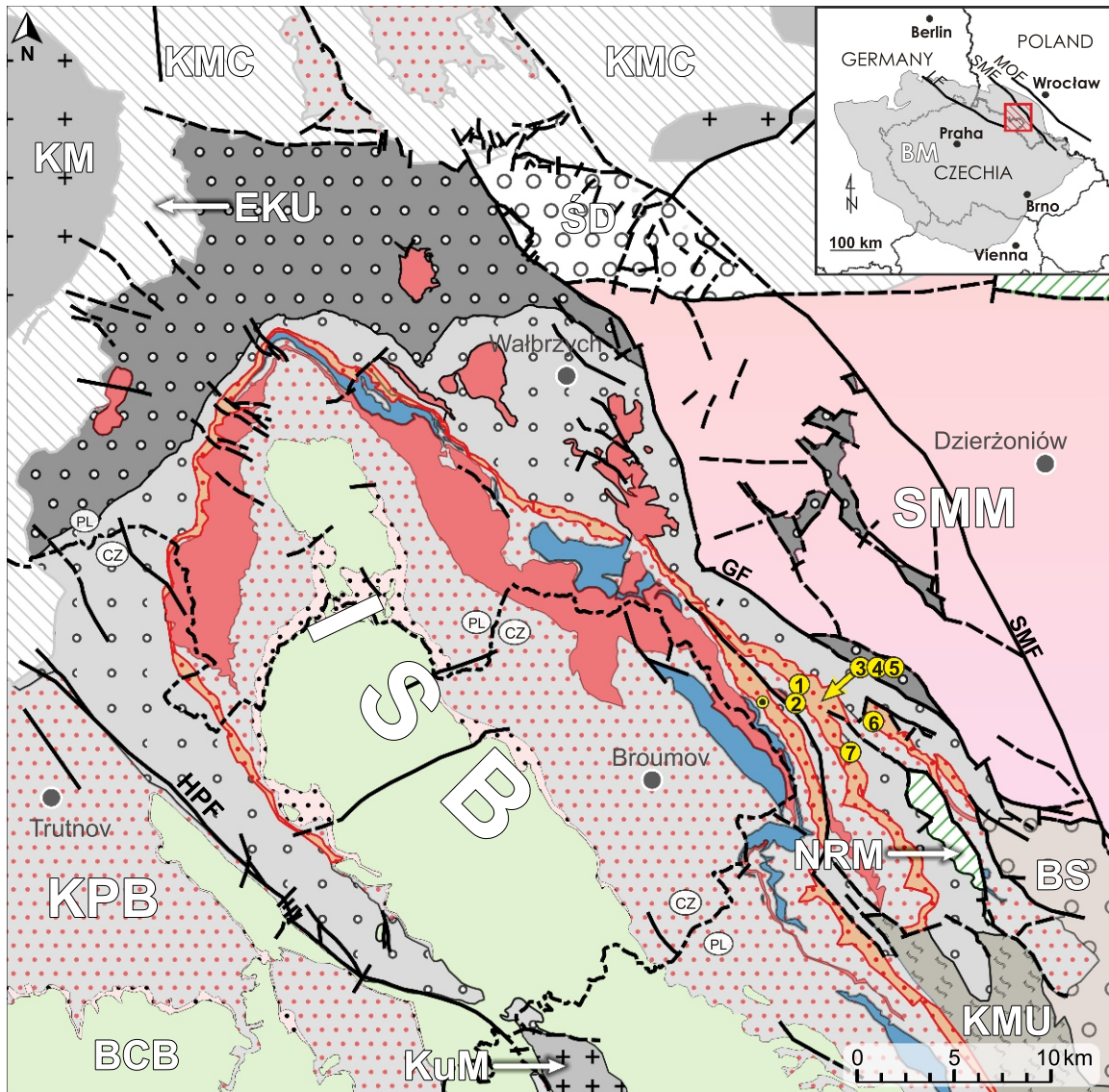


**Fig. 2. Simplified geological map of the Intra-Sudetic Basin with location of main exposures described in the text**

ISB – Intra-Sudetic Basin, ŚD – Świebodzice Depression, SMM – Sowie Mts. Massif, KM – Karkonosze Massif, ECU – Eastern Karkonosze Metamorphic Unit, KMC – Kaczawa Metamorphic Complex, NRM – Nowa Ruda Massif, BS – Bardo Structure, KMB – Kudowa Massif, BCB – Bohemian Cretaceous Basin; important faults: MOF – Middle Odra Fault, LF – Lusatian Fault, SMF – Sudetic Marginal Fault; GF – Głuszyca Fault, HPF – Hronov-Poříčí Fault; geological map based on Sawicki (1995, modified)

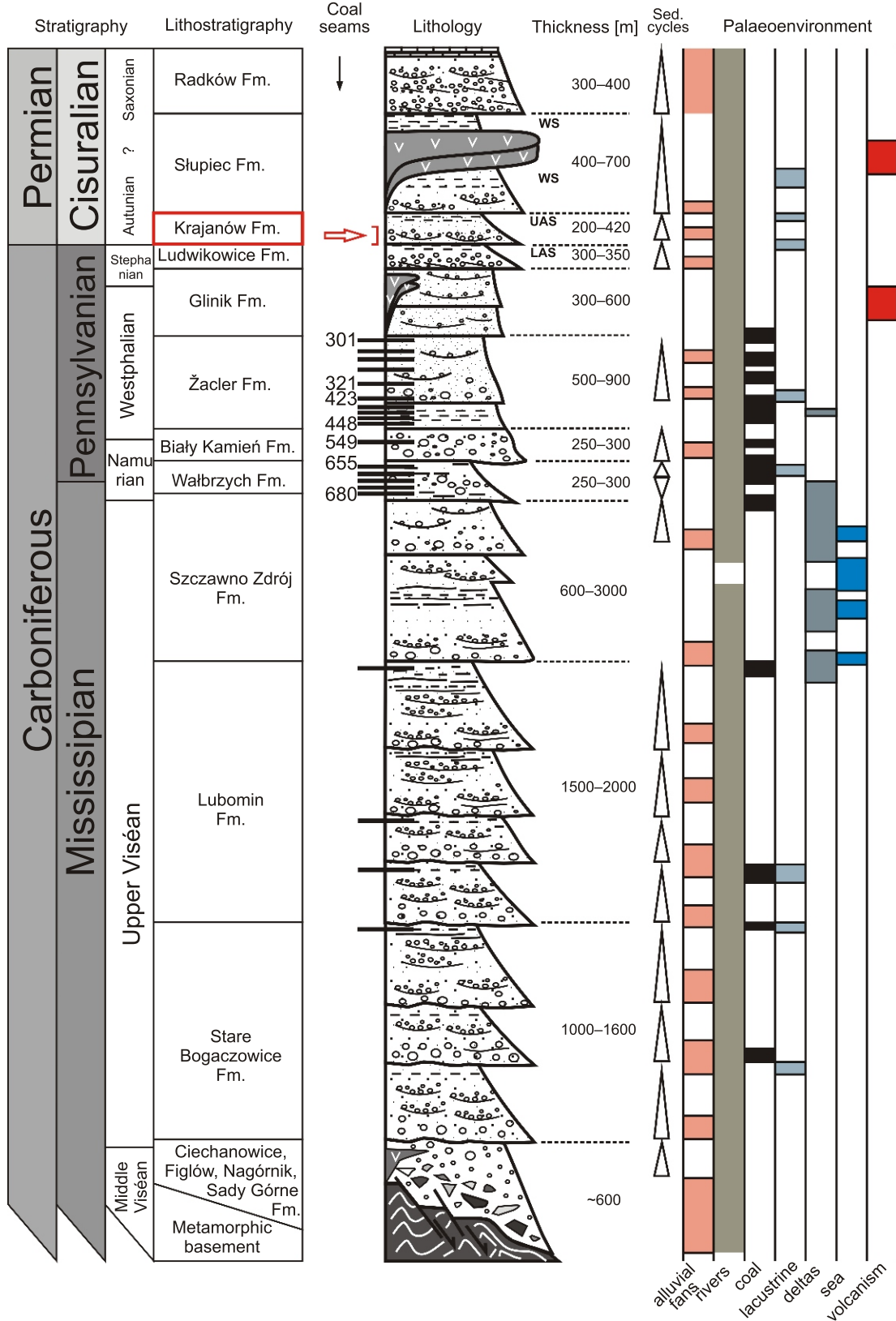


Fig. 3. Synthetic stratigraphic scheme of the Carboniferous and Permian deposits in the Intra-Sudetic Basin

Redrawn from Mastalerz et al. (1993), slightly modified after Turnau et al. (2002) and Górecka-Nowak et al. (2021); LAS – Lower Anthracosia Shale; UAS – Upper Anthracosia Shale; WS – Walchia Shale; red arrow indicates the studied, lowermost interval of the Krajanów Formation

## THE KRAJANÓW FORMATION

Deposits of the Krajanów Formation have been described in geological reports (Dziedzic, 1959, 1961; Don, 1961) and shown on detailed geological maps since the early 20th century (Dathe, 1904a, b; Wójcik, 1958; Gawroński, 1959; Krechowicz, 1964; Krechowicz and Kisielewski, 1965; Cymerman et al., 2015a; Ihnatowicz et al., 2017a). Regional investigations and explanations to geological maps interpreted these deposits typically as fluvial in origin (Don, 1961; Dziedzic, 1961; Krechowicz, 1965; Oberc and Wójcik, 1965; Krechowicz and Berezowska, 1968; Cymerman et al., 2015b; Ihnatowicz et al., 2017b). One of the exposures analysed in this paper (loc. 4) was described by Kurowski (1993, 1995) during conference field trips, but no comprehensive sedimentological study of the Krajanów deposits was conducted.

The stratigraphic position of the Permian deposits in the Intra-Sudetic Basin remains still uncertain and poorly constrained, mainly due to a lack of fossils and poor chronostratigraphic evidence generally. The Krajanów Formation is considered currently as the lowermost lithostratigraphical unit in the Polish part of the Permian Intra-Sudetic Basin. Although the Krajanów Formation has been regarded as lowermost Permian (?Asselian), the real position of the Carboniferous-Permian boundary is still a matter of debate. From palynological studies, the uppermost portion of the underlying Ludwikowice Formation (the so-called Lower Anthracosia Shale) is assigned variously to the lowermost Permian and/or to the uppermost Carboniferous (Górecka, 1981; Jerzykiewicz, 1987; Górecka-Nowak, 1995). The contact between the Ludwikowice and Krajanów formations is probably unconformable and relates probably to a minor depositional gap/unconformity (Don, 1961). The Krajanów Formation is relatively well exposed in its eastern part (the study area), and poorly exposed in the western part of the basin. The lateral stratigraphic equivalent of the Krajanów Formation – the Bečkov Member – is assigned to the uppermost (Autunian or Asselian) part of the Chvaleč Formation in the Czech Republic, in the southwestern part of the Basin (Opluštil et al., 2016). The underlying Vernéřovice Member is a stratigraphic equivalent of the Ludwikowice Formation in the Polish part of the ISB, and is dated as Stephanian C (Gzhelian).

The Krajanów Formation is composed of fluvial, playa-like and lacustrine deposits which form a fining-upwards megasequence up to 420 m in thickness (Mastalerz et al., 1993). Deposits of the lowermost part of the formation are represented by a fluvial red bed assemblage of conglomerates and coarse-grained sandstones which have traditionally been subdivided into two informal lithostratigraphic members: the so-called “lydite conglomerate” in the area between Nowa Ruda and Słupiec to the south-east, and the “quartzite conglomerate” between Nowa Ruda and Świerki to the northwest (Don, 1961). This division was first proposed by early German geologists (Dathe, 1904a, b) based on the petrographic composition of gravel clasts in the conglomerates, and supported also by Don (1961) and Dziedzic (1961). According to the latter authors the two conglomerate members interfinger in the vicinity of Nowa Ruda. According to Mastalerz et al. (1993) and Awdankiewicz et al. (2003) the Krajanów Formation was deposited in a braided fluvial system related to NW–SE elongated palaeovalleys and systems of transverse alluvial fans. Based on the results of sedimentological logging at loc. 4 (see Fig. 2 and the section sedimentary facies and their environmental interpretation in this paper), Kurowski (1993, 1995) stated that deposition of the lowermost Krajanów Formation occurred

“along a very gently inclined sand-mud plain” by a NW-, N- and NE-flowing fluvial system dominated by shallow, wide and frequently shifting alluvial channels.

The middle third of the formation is characterised by fine-grained, reddish-brown sandstones, siltstones and claystones with minor limestone intercalations related to playa-like and ephemeral lake-margin systems. The uppermost part of the Krajanów Formation, distinguished informally as the Upper Anthracosia Shale (Nemec et al., 1982), poorly exposed in proximal to medial regions of the basin, is characterized by mudstone-dominated siliciclastic deposits, representing red to greyish, argillaceous, argillaceous-pelitic and argillaceous-carbonate sediments (Lorenc, 1993). This member accumulated in a floodplain-to-ephemeral (“terminal”) lacustrine setting (Mastalerz and Nehyba, 1997; Kurowski, 2004) during expansion of ephemeral lakes. The deposits are interbedded with fine-grained calcareous deposits, enriched in organic matter and traditionally termed “black shales” (Lorenc, 1993; Nowak, 1998, 2007; Wójcik-Tabol et al., 2021; Nowak et al., 2022). The latter deposits reflect anoxic bottom conditions in the Carboniferous and Permian lakes in the ISB. The vertical and lateral transitions between fluvial and lacustrine systems of the medial to distal setting of the basin are poorly exposed and known mostly from borehole logs (Miecznik, 1989).

## MATERIAL AND METHODS

The region selected for study is situated in the eastern sector of the Intra-Sudetic Basin, built chiefly of Carboniferous and Permian deposits, in the vicinity of Ludwikowice Kłodzkie, Jugów and Nowa Ruda. The lowermost part of the Krajanów Formation is relatively well exposed in this area; exposures include several small, abandoned quarries as well as road and railway cuttings. The succession studied crops out within belts trending NW–SE, parallel or subparallel to the Głuszyca Fault that bounds the present structure of the Intra-Sudetic Basin to the east (Fig. 2).

Sedimentological analysis of the lowermost Krajanów Formation was conducted in 56 selected exposures grouped here into 7 representative sites to characterise the textural and structural features of the deposits and to identify depositional processes. Despite insufficient exposure of the lowermost part of the formation, especially in relation to its bulk thickness (~420 m), a cumulative measured thickness of logged sections reached ~40 m. Sedimentological studies of exposures included macroscopic recognition, description, classification and detailed characterization of lithofacies, as well as vertical logging of the rock texture and sedimentary structures. The maximum particle sizes (MPS) within the individual sedimentary units were recorded. The distinction, description and coding of lithofacies follows a widely used scheme by Miall (1996). Special attention was given to the geometry, arrangement and stacking pattern of sedimentary units, including their lateral and vertical variation. Photomosaics and interpretive sketches were made for the largest exposures with the use of Hugin-Panorama Editor software. Series of photographs were taken with 20–30% overlap between individual shots. Photomosaics were connected with the use of a cylindrical projection which preserves vertical and horizontal lines.

Lithofacies distinguished at sites studied were grouped into architectural elements of a fluvial system according to standardised criteria proposed by Miall (2014) and slightly modified by North and Taylor (1996) for the purposes of ephemeral fluvial system characterisation. The fluvial architectural ele-

ments were grouped into three main categories referred in this paper to as A, B and C. The exposure-scale geometry of the architectural/depositional elements distinguished and their main bounding surfaces are shown in this study on photomosaics and outcrop sketches. We estimated proportions of thickness (%) of the architectural elements distinguished, measured in vertical exposed sections.

Directional palaeocurrent data, based on cross-stratification and palaeochannel axes, were plotted as rose diagrams allowing for the tectonic tilt of the strata. The directions of individual palaeochannel axes and orientations of cross-stratification are shown in the sedimentological logs and were compiled for selected exposures. Macroscopic descriptions of sedimentary units were supplemented with petrographic analysis of gravel-size clasts in selected sections. The individual pebbles, ranging in diameter from 16 to 256 mm, were assigned into classes according to their lithology. For selected lithological varieties, thin-sections were made and analysed with the use of a *Nikon Eclipse LV100N POL* polarizing microscope. Data derived from the sections was complemented with analysis of selected borehole data (Fig. 4), described in detail by Miecznik (1989) and available online from the Polish Geological Survey's National Geological Repository (CBDG).

## RESULTS

### THE KRAJANÓW FORMATION – LITHOLOGY AND PETROGRAPHY

Most of the sections of the lowermost Krajanów Formation studied are dominated by well-cemented, red-brownish to pink and locally red-greyish, cross- and horizontally-stratified sandstones with composite beds of conglomerate (Fig. 5A). Conglomerate lithofacies prevail in the lowermost portion of the unit and in the proximal part of the basin. Sporadic, discontinuous interlayers and intraclasts of dark-brown to reddish mudstone and fine-grained sandstone were observed.

The Krajanów sandstones are arkosic/subarkosic to lithic arenites. Depending on the location, the sandstones differ slightly in the degree of sorting and in the proportions of the petrographic components. The sandstones display a compact framework and low to medium petrographic maturity (Fig. 5B). Most of the components are grains of fine- to medium-grained sand, and subordinately coarse-grained sand. In terms of petrographic composition, more than half of the grains are monocrystalline quartz (57–64%), followed by quartzite (7–24%) and feldspar (9–26%), in places rhyolite grains have a considerable share (6%). The degree of rounding of quartz and feldspar grains is usually low: they are predominantly very angular to sub-angular, occasionally larger grains are sub-rounded (Fig. 5B). Monocrystalline quartz grains exhibit wavy and patchy extinction. The feldspars are mostly beige to light brown, partly kaolinized, some grains have hypautomorphic outlines. Individual grains show polysynthetic twinning. Lithic grains are mostly sub-angular to sub-rounded, while there are individual angular gneiss and rhyolite grains, while a few larger grains of quartzite and rhyolite are rounded. The grain framework is cemented by a ferruginous matrix that gives the rock a characteristic reddish to brownish colour.

The polymictic conglomerates occurring as composite beds within the sandstones are typically clast-supported, less often matrix-supported. A petrographic study (Table 1) carried out in 6 selected locations (loc. nos. 1–4 and 6–7; cf. Fig. 2), shows that the beds of conglomerate are dominated by quartz (32.9% of clasts in total in all locations examined) and quartzite

(31.7%). They are followed by clasts of Carboniferous sandstone (probably those of the underlying Ludwikowice and Glinik formations, 12.7%; cf. Don, 1961). The remaining inventory of the gravel fraction >2 cm consists of lydites (7.5%), rhyolites (6.8%), gneisses (3.6%), muddy to fine-grained sandstone intraclasts (2.2%) and other volcanic rocks (1.3%). Below 1% is the content of volcanic tuff, greenstone and chlorite schist, other metamorphic rocks and gabbro (Table 1). In general, rhyolite and gneiss clasts are angular to subangular, while quartz, quartzite and lydite clasts range from moderate to well rounded (Fig. 5C).

### SEDIMENTARY FACIES AND THEIR ENVIRONMENTAL INTERPRETATION

Twenty-one lithofacies have been distinguished and grouped into three lithofacies associations within the part of the Krajanów Formation studied. They are summarised in Table 2 and shown on representative sedimentary logs from localities nos. 1–4 and 6–7 (Figs. 6 and 7).

#### LITHOFACIES DESCRIPTION AND INTERPRETATION

##### GRAVELLY LITHOFACIES ASSOCIATION

**Clast-supported, massive (Gcm) and graded (Gmg) conglomerates.** This lithofacies typically comprises moderately to well sorted conglomerate with pebble- to cobble-sized clasts up to 20 cm in size (Fig. 8A). The conglomerates are arranged into lenticular or sheet-like, typically amalgamated beds, with thicknesses of 0.1 to 0.6 m. The lower boundaries of beds are always sharp, flat or concave-upwards and erosional, whilst the upper ones are gradational; lithofacies Gcm typically passes upwards into the St/SGt, Sp/SGp, Sm, Sh or Sl lithofacies (Figs. 6 and 7). Clast fabric within conglomeratic beds appears to be chaotic, but locally conglomerates reveal indistinct normal grading (lithofacies Gmg). In the lower parts of beds disc-shaped clasts are locally imbricated (a (t) b (i) fabric; lithofacies Gmg).

**Interpretation.** The conglomerates represent deposits of the bottom, aggradational parts of braided river channels (Collinson, 1996; Bridge, 2009). The lowermost parts of beds composed of the Gcm lithofacies are interpreted as relic deposits of strong, erosive water flow and sediment bypass forming channel-floor lags. The ungraded beds of Gcm facies may include deposits of low-strength, pseudoplastic debris flows entering abandoned (?) braided river channels (Miall, 1996). The thicker beds of Gmg conglomerate with flat bases were deposited as bedload, possibly at the base of unidirectional, high-energy (flood?) flows (Collinson, 1996).

**Horizontally-stratified conglomerates (Gh) and sandy conglomerates (GSh).** Deposits of lithofacies Gh/GSh contain predominantly clast- to matrix-supported conglomerate, poorly to well sorted, dominated by pebble- to cobble-sized clasts. The conglomerate is arranged into discontinuous beds, a few clasts thick, with crude horizontal or nearly horizontal bedding (Fig. 8B, C). Disc-shaped pebbles in the lower parts of beds are usually imbricated (a (t) b (i) fabric). This lithofacies passes typically upwards into the Sm, Sh or Sl lithofacies.

**Interpretation.** Lithofacies Gh/GSh is interpreted to have formed as diffuse gravel sheets (Hein and Walker, 1977) which further accreted into gravel bedforms by vertical/lateral/downstream growth during episodes of high-energy flow and sediment discharge (Rust, 1972; Miall, 1996). Solitary beds of the Gh/GSh lithofacies are interpreted as channel-floor lags.

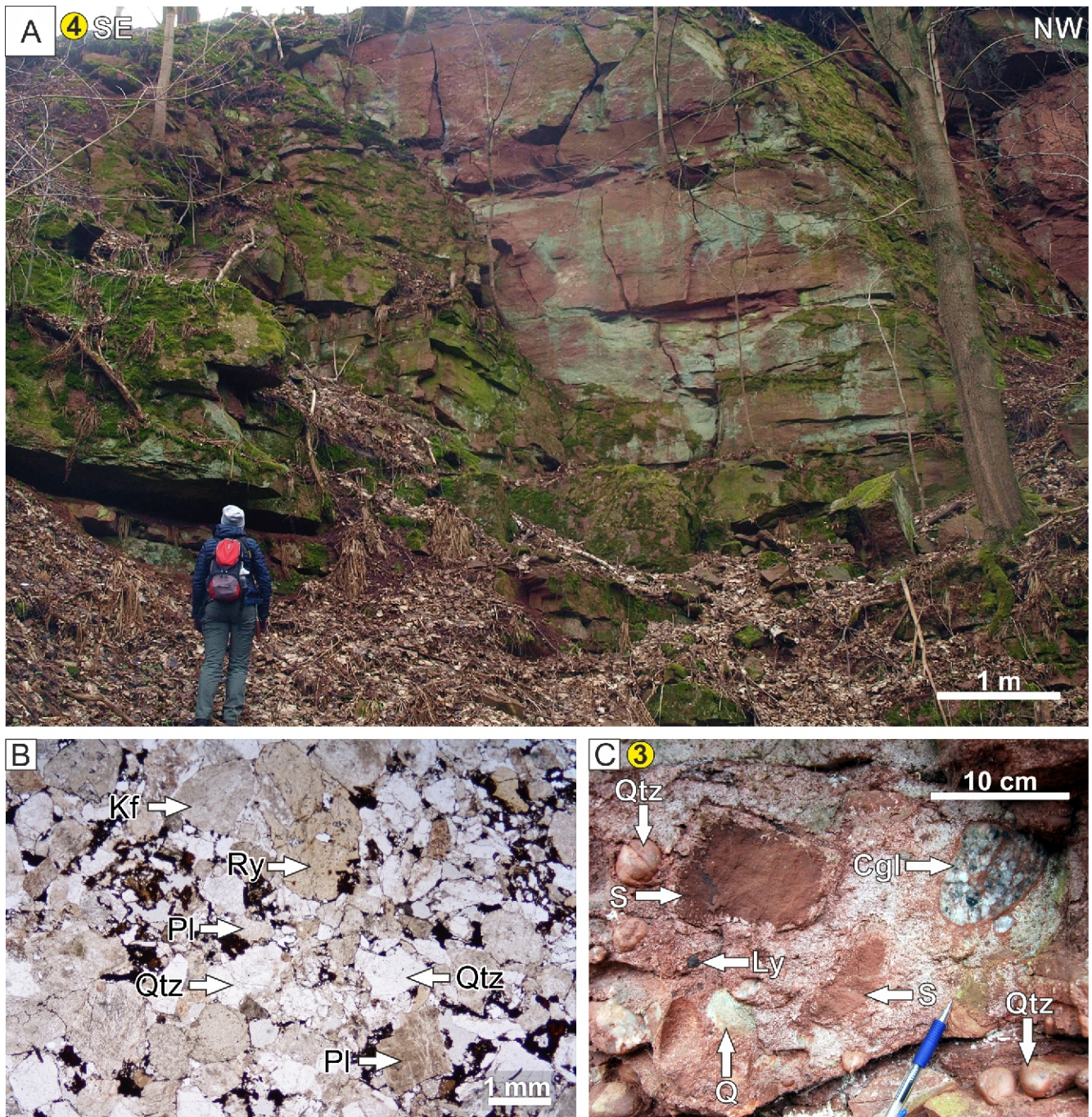


**Fig. 4. Main lithological and petrographic features of the lowermost Krajanów Formation exposed in the eastern Intra-Sudetic Basin**

**A** – repetitively stacked sandstone and conglomerate beds bounded by flat or concave-upwards erosional surfaces (loc. 4); **B** – microscopic view of Krajanów arkose/subarkose to lithic arenite composed mainly of angular to subangular quartz (Qtz), feldspar (Kf), plagioclase (Pl) and rhyolite (Ry) grains cemented by a ferruginous matrix. Note the low petrographic maturity of the sandstone; **C** – conglomerate bed with well-rounded pebbles of lydite (Ly), greenish quartzite (Q), milky quartz (Qtz) and an angular to subrounded clast of reddish-brown sandstone (S)



Table 1

**Lithological composition of gravel clasts from the conglomerates of the lowermost Krajanów Formation**

Lithology	Number of clasts >2 cm	Percent [%]
quartz	378	32.9
quartzite	330	31.7
Carboniferous sandstone	162	12.7
lydite	73	7.5
rhyolite	59	6.8
gneiss	30	3.6
mudstone intraclast	20	2.2
other volcanic	15	1.3
greenstone + chlorite schist	5	0.6
volcanic tuff	5	0.5
other metamorphic	2	0.1
gabbro	1	0.1
total	1080	100

**Matrix supported, massive conglomerates (Gmm).** This lithofacies is composed of poorly to moderately sorted matrix-supported conglomerate (Gmm), typically intraformational (Fig. 8D), which does not display any internal structure (Fig. 8E). The clasts are supported by a poorly sorted matrix of medium- to coarse-grained sand. Beds of conglomerate are up to 0.3 m thick, and are laterally discontinuous/lens-shaped. The lower and upper boundaries of beds are typically sharp but non-erosional. Bases of Gmm beds are locally loaded (Fig. 8E) and display more complex, soft-sediment deformation structures (Fig. 8F). The latter include isolated, loaded angular clasts of matrix-supported conglomerate, up to 20 cm in length, accompanied by silty to clay matrix injected from the underlying strata.

**Interpretation.** The Gmm lithofacies is interpreted as deposits of high-strength debris-flows supported by pore fluid pressure/cohesion and dispersive pressure (Collinson, 1996; Miall, 1996). This lithofacies represents gravity flow sheets and lobes which entered pre-existing alluvial channels (Miall, 1996). Soft-sediment deformation structures and load structures developed within lithofacies Gmm are interpreted as a result of bank collapse in an active river channel (e.g., Priddy et al., 2021).

**Planar cross-stratified conglomerates (Gp) and sandy conglomerates (GSp).** Deposits of the lithofacies Gp/GSp contain clast- to matrix-supported, poorly sorted conglomerate dominated by granule to cobble-sized clasts. The conglomerate is arranged into planar (tabular) cross-stratified sets bounded by nearly flat, sharp erosional surfaces (Fig. 8G). Cross-stratified bed sets are relatively thin, range in thickness between 0.2 and 0.4 m and are up to several metres wide. The planar cross-stratified sets contain pseudo-imbricated, dark-brown or reddish sandstone intraclasts, up to 10 cm long.

**Interpretation.** Lithofacies of Gp/GSp were formed under unidirectional aqueous currents during migration of straight-crested, 2D gravelly dunes as midchannel transverse or linguoid bedforms (Miall, 1977).

**Trough cross-stratified conglomerates (Gt) and sandy conglomerates (GSt).** Deposits of this lithofacies typically comprise poorly to moderately sorted, clast- to matrix-supported conglomerate dominated by the pebble- to cobble-sized fraction supported by a coarse-grained sand matrix. Gravel clasts are up to 24 cm in diameter. The internal architecture of

the Gt/GSt lithofacies comprises lenticular beds with a thickness of 0.2 to 0.5 m, with sharp, erosional concave-up bases (Fig. 8H). The upper boundaries of beds are gradational. In the lower parts of beds, clasts are sporadically imbricated.

**Interpretation.** This lithofacies formed under unidirectional water currents during migration of sinuous-crested, 3D gravelly dunes as midchannel transverse bedforms (Harms et al., 1975; Collinson, 1996). Locally, deposits of lithofacies Gt and GSt may represent infills of minor channels (Miall, 1977)

## SANDY LITHOFACIES ASSOCIATION

**Massive sandstones (Sm).** Deposits of this lithofacies comprise medium- to coarse-grained, poorly to moderately sorted sandstone with scattered sub-rounded and well-rounded granule- to pebble-sized clasts. Macroscopically, beds of sandstone do not display any internal structures and appear to have been homogenized (Fig. 9A). They typically overlie conglomerate of Gcm lithofacies or underlie the Gh/GSh lithofacies. The beds of sandstone display medium- to large-scale lenticular geometry with lateral extents of up to 2 m. The beds range in thickness between 0.2 and 0.4 m.

**Interpretation.** The massive, internally homogenized ("structureless") sandstones are interpreted as the result of a sudden discharge of transported clastic material, probably from rapid suspension fallout (Horn et al., 2018; Kędzior and Popa, 2018). Massive sandstones may be also related to rapid collapse of a subaqueous sandy bedform and/or sediment fluidization.

**Large-scale cross-stratified sandstones and conglomeratic sandstones (Sl, SGI).** This lithofacies consists of medium- to very coarse-grained, moderately sorted sandstone with scattered sub- to well-rounded granule- to cobble-sized grains. The sandstones are arranged into low-angle, planar cross-stratified bed sets, a few metres wide and up to 1 m thick. The dip of low-angle foresets varies from 3 to 15°, but commonly is <10°. Bases of the beds are predominantly gradational (Fig. 8E, F).

**Interpretation.** The low-angle cross-stratified sandstones are interpreted as washed-out dunes and/or antidunes, which generally formed at the transition from subcritical to supercritical unidirectional flow (Miall, 1996; Kędzior and Popa, 2018).

**Horizontally to subhorizontally stratified sandstones (Sh).** Deposits of lithofacies Sh comprise medium- to coarse-grained, red to pink sandstone with scattered sub- to well-rounded granule-sized grains. The sandstone is typically moderately to well sorted. The lithofacies is characterized by flat or nearly flat or low angle (<5°) parallel lamination ranging in thickness between 2 mm and 5 mm, arranged into tabular sets up to 0.2 m-thick (Fig. 9A, B). Sets of Sh lithofacies display laterally extensive, either flat or irregular, non-erosional bases and tops. The lateral extent of beds reaches a few metres or may exceed the exposure limits. In loc. nos. 2 and 7, horizontally stratified sandstones are underlain by conglomerates of lithofacies Gcm or Gh which infill shallow, trough-shaped erosional scours (Fig. 8B). On the upper bedding planes of horizontally stratified sandstones, primary current lineation is visible (Fig. 9A). Obstacle scours related to pebbles resting on the upper bedding planes have been also observed. Some deposits of lithofacies Sh contain discontinuous and thin (up to 2 mm) intrasets of dark brown mudstone (facies Fm/FSm) to fine-grained sandstone draped with a micaceous film (Fig. 9B).

**Interpretation.** Lithofacies Sh, with parting lineation and current crescent scours on bedding planes, reflects high stream energy (Harms et al., 1975). This lithofacies was depos-

Summary of lithofacies distinguished within the lowermost Krajanów Formation

Facies associations	Lithofacies	Lithology and texture	Sedimentary structures and other features	Interpretation
Gravelly lithofacies association (A)	Gcm, Gmg	Clast-supported, massive (Gcm) and graded (Gmg) conglomerates, moderately- to well-sorted	Structureless (Gcm) or crude normal grading (Gmg), imbrication and pebble alignment in the lower parts of beds	Deposits of bottom, aggradational parts of braided river channels (Gcm, Gmg), and/or deposits of low-strength, pseudoplastic debris flows (Gcm) entering abandoned (?) braided river channels (Miall, 1996; Collinson, 1996)
	Gh, GSh	Clast- to matrix-supported conglomerates, poorly to well sorted, scattered muddy and sandy intraclasts	Crude horizontal or nearly horizontal stratification. Imbricated pebbles in the lower parts of beds (a (t) b (i) fabric)	Diffuse gravel sheets (Hein and Walker, 1977). Relic deposits of strong, erosive water flow and sediment bypass forming channel-floor lag (Rust, 1972; Miall, 1996)
	Gmm	Poorly to moderately sorted, matrix-supported conglomerate, typically intraformational. Clasts supported by a poorly sorted matrix of medium- to coarse-grained sand	Lack of any internal structure, non-erosional, sharp boundaries of beds	Deposits of high-strength debris-flows supported by pore fluid pressure/cohesion and dispersive pressure (Collinson, 1996). Gravity flow sheets and lobes entering pre-existing alluvial channels (Miall, 1996)
	Gp, GSp	Clast- to matrix-supported, poorly sorted conglomerate dominated by granule to cobble-sized clasts	Planar (tabular) cross-strata sets bounded by nearly flat, sharp erosional surfaces. Pseudo-imbricated, dark-brown or reddish sandstone intraclasts, up to 10 cm in length	Migration of straight-crested, 2D gravelly dunes as a transverse or linguoid bedforms (Harms et al., 1975; Miall, 1977)
	Gt, GSt	Poorly to moderately sorted, clast- to matrix-supported conglomerate dominated by pebble- to cobble-sized fraction	Lenticular beds with a thickness of 0.2 to 0.5 m, sharp, erosional concave-up bases. The upper boundaries gradational. In the lower parts of beds imbricated clasts (a (t) b (i) fabric)	Migration of sinuous-crested, 3D gravelly dunes as a transverse bedforms (Harms et al., 1975; Miall, 1977)
Sandy lithofacies association (B)	Sm	Medium- to coarse-grained, poorly to moderately sorted sandstone with scattered sub-rounded and well-rounded granule to pebble-sized clasts.	Lenticular geometry of beds with lateral extent of up to 2 m and thickness between 0.2–0.4 m. Lack of internal structure.	Sudden discharge of transported clastic material, probably from rapid suspension fall out from a traction carpet (Horn et al., 2018; Kędzior and Popa, 2018) and/or rapid collapse of a subaqueous sandy bedform, sediment fluidization.
	Sl, SGI	Medium- to very coarse-grained, moderately sorted sandstones with scattered sub- to well-rounded granule to cobble-sized grains	Low-angle, planar cross-stratified bed sets, a few metres wide and up to 1 m thick. The dip of low-angle foresets from 3 to 15°, commonly <10°. The bases of beds predominantly gradational	Washed-out dunes and/or antidunes, formed at the transition from subcritical to supercritical unidirectional flow (Miall, 1996; Kędzior and Popa, 2018)
	Sh	Fine to coarse-grained sandstones, moderately to well sorted, scattered granules	Parallel or nearly parallel horizontal stratification, tabular sets of up to 0.2 thick, laterally extensive, either flat or irregular, non-erosional bases and tops	Plane-bed transport in the upper flow regime conditions, at the transition from subcritical to supercritical flow (Harms et al., 1975), flow velocities of ~1 m/s and depths of 0.25–0.5 m (Miall, 1996). Individual bed of the Sh interpreted as a result of single, flash flood event (Miall, 1996)
	Sx	Fine to medium-grained sandstones, moderately to well sorted	Low-angle, nearly symmetrical/undulating laminae arranged into cross-stratified bed sets with flat erosional bases. The thickness of up to 15 cm	Propagation of nearly symmetrical, low-amplitude antidunes under supercritical flow conditions. High rates of aggradation (Cartigny et al., 2014)
	St, SGt	Medium- to coarse-grained sandstones with dispersed, subangular to well-rounded granule to pebble-sized clasts	Trough cross-stratification, pseudoimbrication of scattered pebbles resting on bedform lee side, reactivation surfaces	Migration of sinuous-crested, linguoid or crescentic 3D sandy dunes, forming mid-channel bars or their core parts. Upper limits of the lower flow regime, deposition under unidirectional, aqueous currents (Miall, 1977; Leclair and Bridge, 2001)
	Sp, SGp	Medium- to very coarse-grained, poorly to moderately sorted sandstone with dispersed, sub-rounded and well-rounded granule to pebble-size clasts. Scattered reddish and purple sandy intraclasts, abundant locally	Planar cross-stratification, pseudoimbrication of scattered pebbles resting on bedform lee side, low-angle reactivation surfaces	Migration of straight-crested, 2D dunes accreted to midchannel bars or acting as transverse/oblique unit bars. Deposition under medium part of lower-flow regime under unidirectional aqueous currents (Collinson, 1970; Miall, 1977)
	Sr	Very fine to medium-grained, well-sorted sandstone	Asymmetrical ripple cross-lamination; undulatory and linguoid ripple forms. Cross-laminated sets with a thickness from 2 cm to 6 cm, the lamination occasionally marked by admixture of silt	Migration of subaqueous, ripple-scale, linguoid bedforms in the lowermost part of the lower flow regime, under unidirectional current. Ripples migrated at low flow speed (<1m/s) (Miall, 1996)
Muddy lithofacies association (C)	Fm, FSm	Dark brown to reddish-brown mudstones with sporadic intercalations of very fine- to fine grained, red-pinkish sandstone	Massive structure, the sandy mudstones occasionally reveal horizontal lamination. Discontinuous lenses and sheets which range in thickness from 2 mm to 20 cm and widths of a few metres. The lower boundaries are predominantly gradational, whilst the upper ones are often erosional. Discontinuous lenses at the bases of fluvial palaeochannels. Locally bioturbated	Deposition from suspension in local depressions in floodplain ephemeral ponds/lakes. Channel abandonment and its subsequent drying



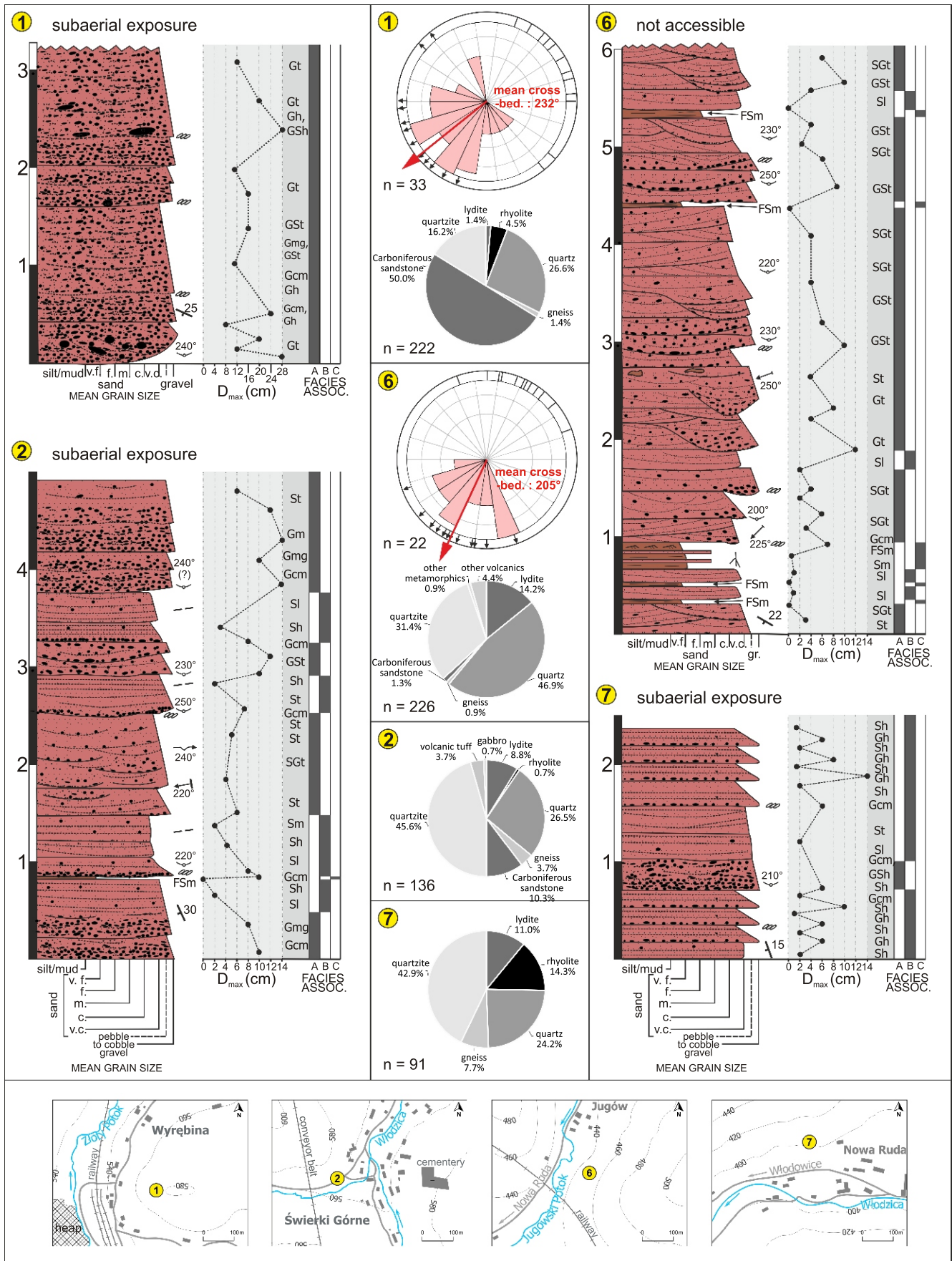
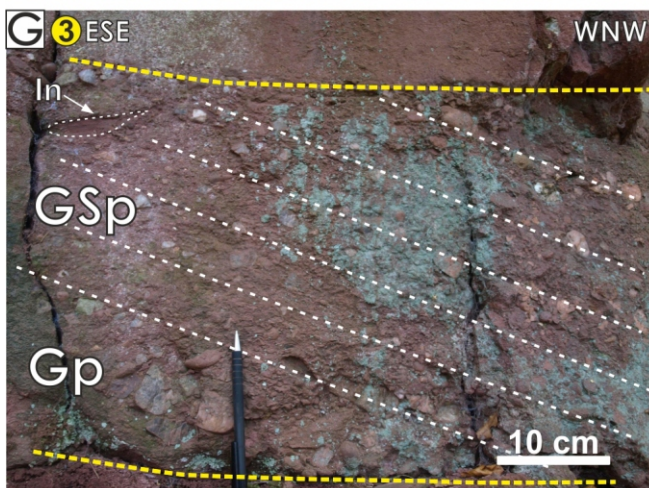
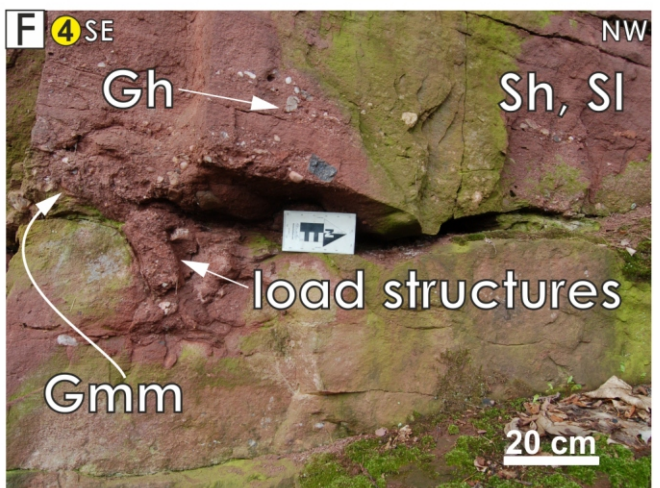
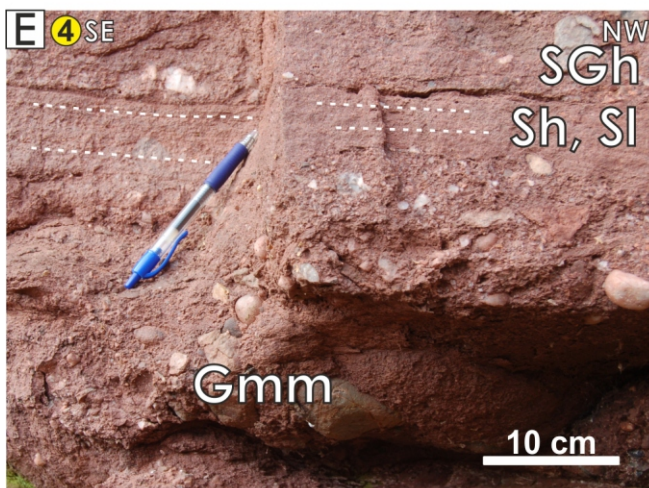
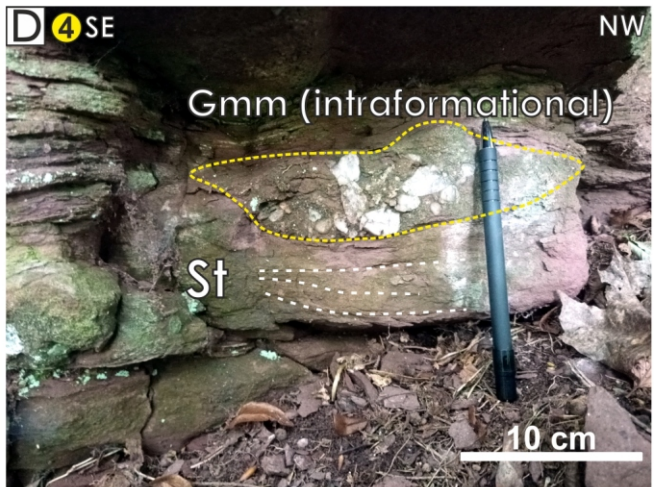
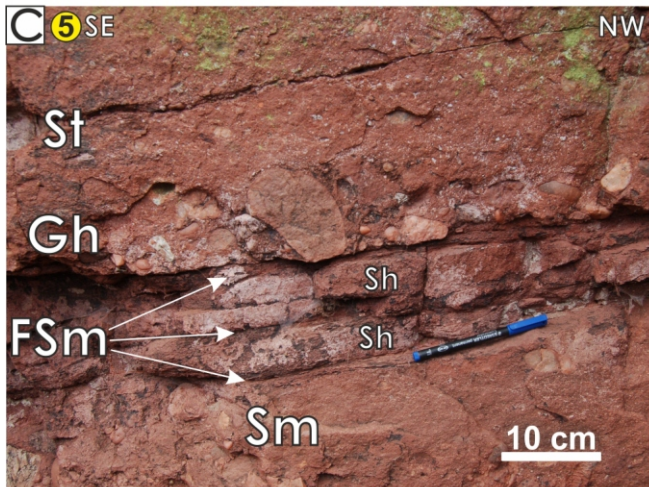
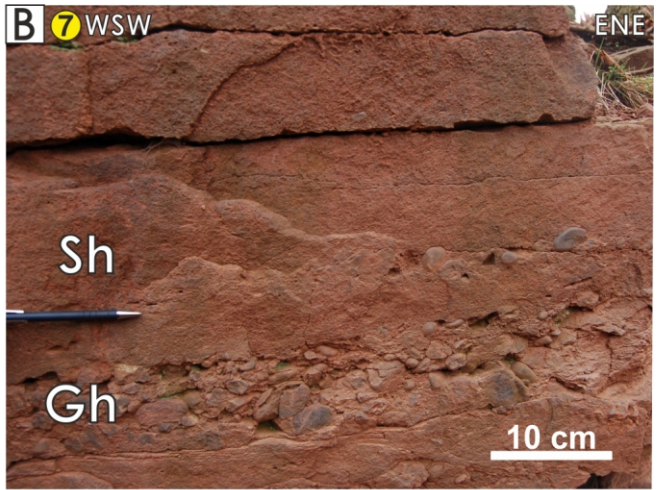


Fig. 7. Sedimentological logs from selected exposures (localities 1, 2, 6, 7) in the eastern Intra-Sudetic Basin, with sedimentary facies indicated (letter code as in Table 2 and in the text)

For other explanations see Figure 6



ited under upper flow regime conditions, at the transition from subcritical to supercritical flow (Bridge and Best, 1988), with flow velocities of ~1 m/s and depths of 0.25–0.5 m (Miall, 1996). Primary current lineation, oriented parallel to flow, is a result of the “streaky” structure of the viscous sublayer (Allen, 1982; Bridge, 2009). Individual beds of the Sh lithofacies are interpreted as deposits of single, flash flood events (Miall, 1996). Plane-bed transport in the upper flow regime included sheet floods in overbank and inter-channel areas.

**Sandstone with small-scale sigmoidal cross-stratification (Sx).** Deposits of lithofacies Sx comprise fine to medium-grained, moderately to well sorted sandstone. The lithofacies is characterised by low-angle, nearly symmetrical/undulose laminae arranged into cross-stratified bed sets with flat erosional bases (Fig. 9C). The beds reach a thickness of up to 15 cm. The Sx lithofacies is typically followed by Fm and FSm lithofacies.

**Interpretation.** Facies Sx records propagation of nearly symmetrical, low-amplitude antidunes formed in supercritical flow conditions with Froude numbers  $1.0 < 1.8$  (Cartigny et al., 2014). Such antidunes generally have stationary crests and troughs, developing in-phase with the water surface during flash flood conditions. Preservation of symmetrical bedforms suggests high rates of aggradation.

**Trough cross-stratified sandstones (St) and conglomeratic sandstones (SGt).** Deposits of the St/SGt lithofacies contain medium- to coarse-grained, poorly to moderately sorted sandstone with dispersed, subangular to well-rounded granule- to pebble-sized clasts. Trough cross-stratified bed sets are characterized by lenticular geometry, concave-up erosive bases and flat or nearly flat tops. The bed sets range in thickness between 0.1 and 0.5 m and their lateral extent reaches a few metres (Fig. 9D). The trough cross-stratified sandstones are commonly interbedded with fine-grained sandstones containing mudstone and siltstone interlayers (lithofacies FSm and SFm). Reddish and purple rip-up intraclasts composed of fine sand occur locally in the tops of beds.

**Interpretation.** Lithofacies St/SGt is interpreted as reflecting the migration of sinuous-crested, linguoid or crescentic 3D sandy dunes, that formed mid-channel bars or their core parts. These lithofacies were deposited in the upper limits of the lower flow regime under unidirectional water currents (Miall, 1977).

**Planar cross-stratified sandstones (Sp) and conglomeratic sandstones (SGp).** Deposits of lithofacies Sp and SGp contain medium- to very coarse-grained, poorly to moderately sorted sandstone with dispersed, sub-rounded and well-rounded granule- to pebble-sized clasts. Cross-stratified bed sets reveal medium- to large-scale lenticular geometry with lateral extents of up to 4 m that are bounded by nearly flat, erosional surfaces (Fig. 9D). Scattered reddish and purple sandy intraclasts are locally abundant, especially at the bases of cross-stratified sets. The bed sets range in thickness between 0.2 and 0.5 m. Planar cross-strata sets, especially at locality 4, show internal low-angle reactivation surfaces.

**Interpretation.** Facies Sp and SGp were formed during migration of straight-crested, 2D dunes accreted to midchannel bars or acting as transverse/oblique unit bars within the central part of the lower-flow regime (Miall, 1977). The facies was deposited under unidirectional water currents; cross-stratified bed sets formed by lee-side avalanching of sand on foresets near the angle of repose (~15–30°; Miall, 1996). Low-angle reactivation surfaces point to changes in river water stage over dunes (Collinson, 1970).

**Ripple-laminated sandstones (Sr).** Deposits of lithofacies Sr contain very fine to medium-grained, red-brownish to pink, moderately to well sorted sandstone. The deposit is arranged into multiple, asymmetrical ripple cross-laminated sets with thicknesses from 2 to 6 cm (Fig. 9E). The lamination occasionally includes an admixture of silt. Cross-stratified bed sets reveal small- to medium-scale lenticular geometry and lateral extents of up to 2 m. The lower and upper bounding surfaces are mainly gradational. The Sr lithofacies is typically followed by Fm and FSm lithofacies or occur as interlayers within deposits of FSm lithofacies.

**Interpretation.** Lithofacies Sr formed during migration of subaqueous, ripple-scale, linguoid bedforms in the lowermost part of the lower flow regime, under unidirectional currents. Ripples migrated at low flow speeds (<1m/s) (Miall, 1996).

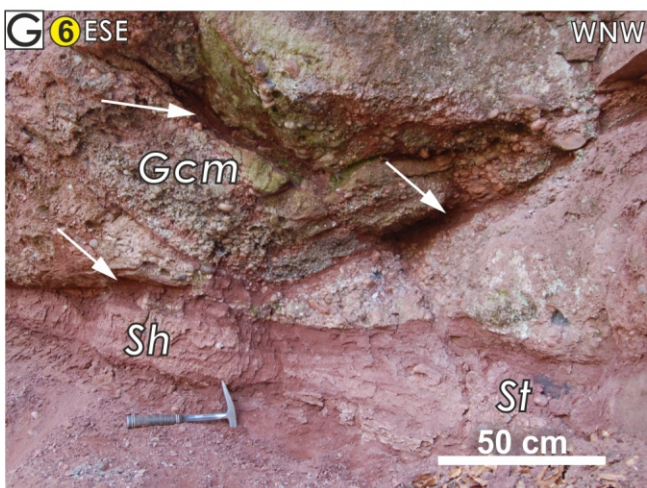
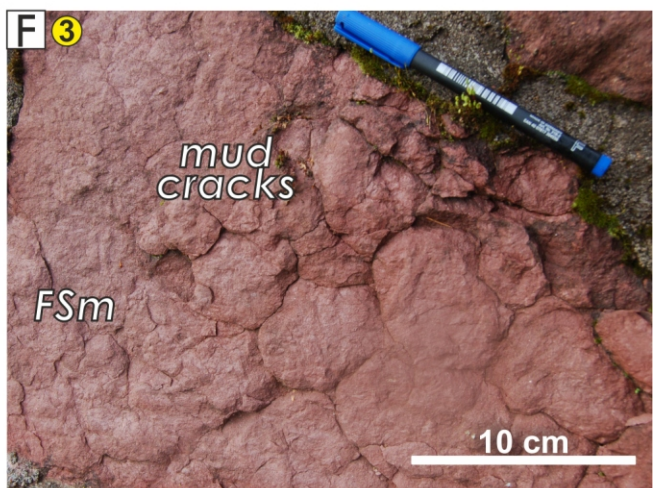
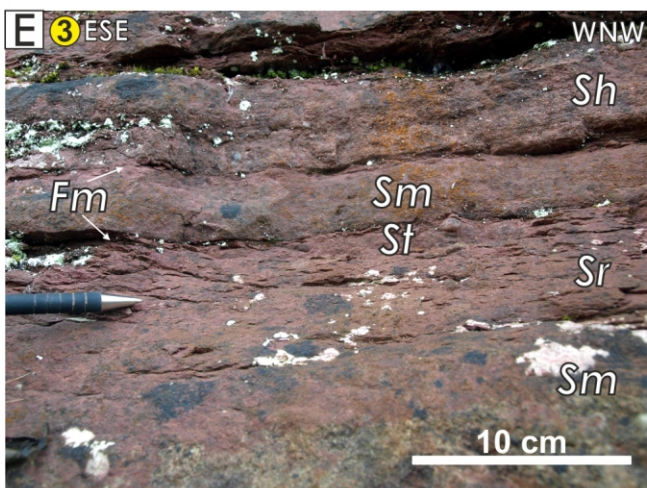
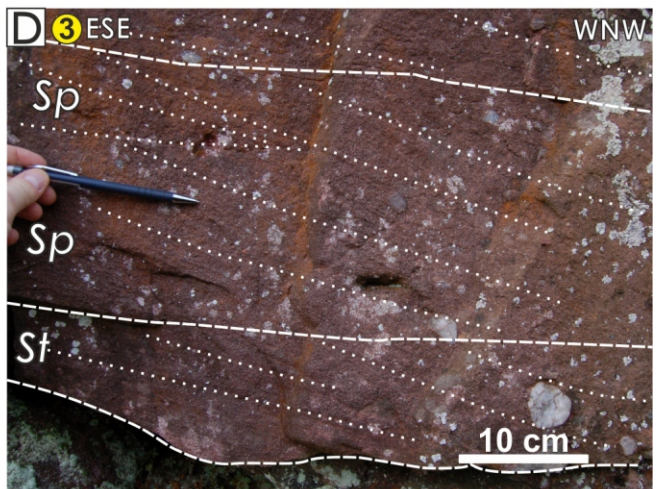
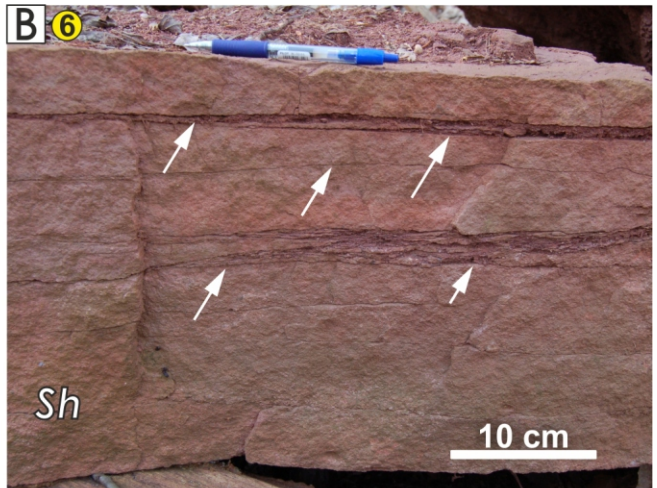
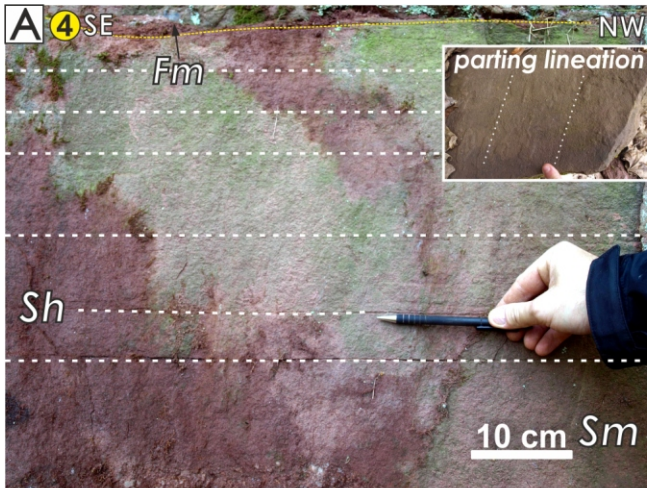
#### MUDDY LITHOFACIES ASSOCIATION

**Massive mudstones (Fm) and sandy mudstones (FSm).** Deposits of lithofacies Fm/FSm contain dark brown to reddish-brown mudstones with sporadic intercalations of very fine- to fine-grained, red-pinkish sandstone. The mudstones display a massive structure, though the sandy mudstones may occasionally reveal horizontal lamination. These deposits form discontinuous lenses and sheets, mainly in the tops of St and Sh lithofacies, which range in thickness from 2 mm to 20 cm and attain widths of a few metres. The dark mudstones occur also as thin interlayers within the St and Sh lithofacies (Fig. 9B). The lower boundaries of the FSm/Fm lithofacies are predominantly gradational, and the upper ones commonly erosional. Mud cracks were observed on the upper bedding surfaces of sandstones of the Sh lithofacies at loc. 3 (Fig. 9F). Reddish-brown, fine-grained sandstones and mudstones were observed also as discontinuous lenses, up to 3 cm thick, at the bases of fluvial palaeochannels (Fig. 9G). The mudstones are locally bioturbated. Bioturbation was observed mainly on the upper bedding planes of sandstone blocks as polygonal systems of anabranching tunnels, oval in cross-section (Fig. 9H). This lithofacies constitutes a subordinate (up to c. 8%) component of the lowermost Krajanów Formation.

**Interpretation.** Lithofacies Fm/FSm is interpreted to be deposited from suspension in local depressions formed in floodplain ephemeral ponds/lakes. The muddy to fine sandy capping of the channels represents channel abandonment and its subsequent drying. Bioturbation is represented by plant root

**Fig. 8. Sedimentary features of the lowermost Krajanów Formation exposed in the eastern Intra-Sudetic Basin (gravelly lithofacies association)**

**A** – clast-supported, massive conglomerate of the Gcm lithofacies; **B** – horizontally stratified conglomerate overlain by horizontally stratified sandstone of lithofacies Sh; **C** – horizontally stratified conglomerate underlain by Sh sandstone interbedded with fine-grained deposits of lithofacies FSm; **D** – intraformational conglomerate with no internal structure (Gmm lithofacies); **E** – discontinuous bed of matrix-supported conglomerate (lithofacies Gmm) with sharp, loaded base; **F** – distinct load structures and soft-sediment deformation structures at the base of a bed of matrix-supported conglomerate (lithofacies Gmm); **G** – conglomerate (lithofacies Gp) and sandy conglomerate (lithofacies GSp) with planar cross-stratification; **H** – conglomerate with trough cross-stratification (lithofacies Gt)



traces and burrows formed by invertebrates. Trace fossils, assigned to *Scoyenia* ichnofacies, were described by (Kiersnowski et al., 2021) from the overlying, fluvial Słupiec Formation in the Intra-Sudetic Basin. Single, unbranched burrows probably represent *Planolites* sp.

#### FLUVIAL ARCHITECTURAL ELEMENTS AND THEIR ENVIRONMENTAL INTERPRETATION

The lithofacies distinguished have been grouped into three major architectural elements of an early Permian (?Asselian) fluvial system (as defined by Teisseyre, 1991 and Miall, 2014) of the eastern Intra-Sudetic Basin. The following architectural elements: (A) amalgamated fluvial channel infills with sediment gravity flow deposits and bank collapse elements (CHa), (B) poorly channelized to non-channelized fluvial sheet-like elements (LS) and (C) overbank fines (FF), are related genetically to distinct fluvial depositional sub-environments.

##### (A) Amalgamated fluvial channel infills (CHa) with sediment gravity flow deposits and bank collapse elements

These architectural elements consist of gravel-dominated lithofacies of Gcm, Gmg, Gmm, Gh/GSh, Gp/GSp and Gt/GSt, as well as sand-dominated lithofacies of Sp/SGp, St/SGt, and less common Sm. In the study area, CHa elements prevail in the lowermost Krajanów Formation and in the proximal regions of the eastern Intra-Sudetic Basin (loc. nos. 1, 2; Fig. 10A). In the localities studied the lithofacies are arranged into vertically stacked and amalgamated, cross-cutting sheet-like bodies with a concave-upwards geometry. The lower boundaries of these elements are often sharp (erosional). In vertical sections, the measured proportion of the total thickness (%) of the CHa elements range from 53% in the more distal regions of the basin (loc. 3; Fig. 10B) to nearly 100% in the proximal region (loc. 1; Fig. 10A).

The CHa elements are interpreted as palaeochannels of a multi-storey, non-perennial to ephemeral braided fluvial system. Basal channel-floor lags of lithofacies Gcm typically pass gradationally upwards into cross-stratified units of Gp/GSp, Gt/GSt and/or Sp/SGp and St/SGt. Preserved sheets of fine-grained, dark-brown sandstone resting on the basal surfaces of channels at loc. 6 point to periodic channel dryness and, subsequently, their rapid infill, probably during occasional, catastrophic flash floods. The trough and planar cross-stratified lithofacies point to migration of 3D and 2D dunes within the channels (Harms et al., 1975). These forms developed as a variety of small, mid-channel gravelly and sandy bars (e.g., Miall, 1977; Collinson, 1996) under lower flow regime conditions. During stages of low sediment load, the bedforms were probably partially emergent and vegetated. Structureless (massive) sandstones of lithofacies Sm, observed at locs. 2, 3 and 5, reveal rapid in-channel deposition from high-energy flows that prevent in-channel bedform development. The occurrence of Gmm lithofacies points to gravity flow deposits which entered

alluvial channels during flash floods (Miall, 1996) or formed due to the collapse of river banks. The spatial trend of palaeochannels, and the measured, internal palaeoflow directions, indicate consistent sediment transport towards the west, southwest and northwest, nearly perpendicular to the present-day tectonic boundaries of the Intra-Sudetic Basin.

##### (B) Poorly channelized to non-channelized fluvial sheet-like elements (LS)

These architectural elements consist of sandstone-dominated Sl/SGl, Sh, Sx and Sr lithofacies. In the sections studied these lithofacies formed laterally extensive, non-channelised or poorly channelised sheets which typically overlie conglomerates of Gcm or Gmg lithofacies and cross-stratified units of Gp/GSp, Gt/GSt as well as Sp/SGp and St/SGt lithofacies (Fig. 10B). In vertical sections, the measured proportions of the total thickness (%) of these elements range from ~11% in the proximal regions of the basin (loc. 6) to nearly 41% in the more distal regions of the basin (loc. 3). LS elements predominate at loc. 7 (88%); however, due to the limited size of the exposure, this value cannot be considered as representative.

These laterally pervasive elements are interpreted as deposits of unconfined sheet flows and/or erosional remnants of wide and shallow channels. The Sh lithofacies with planar erosional bases points to very shallow, high-energy flows. The occurrence of Gcm underlying Sl/SGl, Sh lithofacies support this notion. The presence of discontinuous intrasets of dark brown mudstone of lithofacies Fm/FSm, also with mud cracks, within this lithofacies, suggest waning flood flows and subsequent drying of the sediment surface. Non-channelized sheet-like bodies, composed mainly of Sh, Sm and minor Sx lithofacies extend laterally beyond the limits of the exposures studied. Interpreted rapid flows in the upper flow regime probably extended laterally beyond the channel margins as sheet floods.

##### (C) Overbank fines (FF)

These architectural elements consist of mud-dominated, Fm/FSm as well as sandy Sr lithofacies. In the sections studied, these deposits form either laterally discontinuous sheets and lenses in the top of CHa and LS elements or occur as isolated lenses within channels filled with Gcm and Gmg lithofacies. The first of these fine-grained deposits are typically incised by conglomerate bodies of CHa elements. In vertical sections, the measured proportions of the total thickness (%) of the FF elements range from <1% in the proximal regions of the basin (loc. 1, 2) to nearly 8% in the more distal regions (loc. 3).

The FF architectural elements are interpreted as (i) deposits of overbank and/or adjacent floodplain environments and (ii) as an effect of channel abandonment and its subsequent drying. Overbank and floodplain environments in the study area were dominated by deposition from suspension fallout in standing water of ephemeral ponds and small lakes (Fig. 10A). Less abundant, horizontally laminated sandy mudstones are related to short-lived events of unconfined flows and suspension

Fig. 9. Sedimentary features of the lowermost Krajanów Formation exposed in the eastern Intra-Sudetic Basin (sandy and muddy lithofacies associations)

**A** – sandstone with horizontal stratification (lithofacies Sh, vertical exposed section, locality 4) and parting lineation visible on the upper bedding surfaces in loose block at locality 4; **B** – thin interlayers of lithofacies Fm/FSm (arrowed) within sandstone with horizontal stratification (Sh); **C** – sandstone with clearly visible, small-scale sigmoidal cross-stratification (Sx) underlain by lithofacies Sh and Sm, bounded by sharp, nearly planar erosional surfaces; **D** – stacked sandstone beds with trough (St) and planar cross-stratification (Sp) bounded by concave-upwards and planar erosional surfaces; **E** – fine- to medium-grained, ripple-laminated sandstones of lithofacies Sr, underlain and overlain by lithofacies Sm; **F** – polygonal mud cracks preserved on the upper bedding surface of sandy mudstone (FSm) in a loose block at locality 3; **G** – discontinuous lenses of fine-grained sandstone and mudstone (lithofacies FSm) occurring at the bases of and within fluvial palaeochannels filled with Gcm lithofacies; **H** – bioturbation structures in the form of solitary, curved burrows observed in a loose block at locality 3

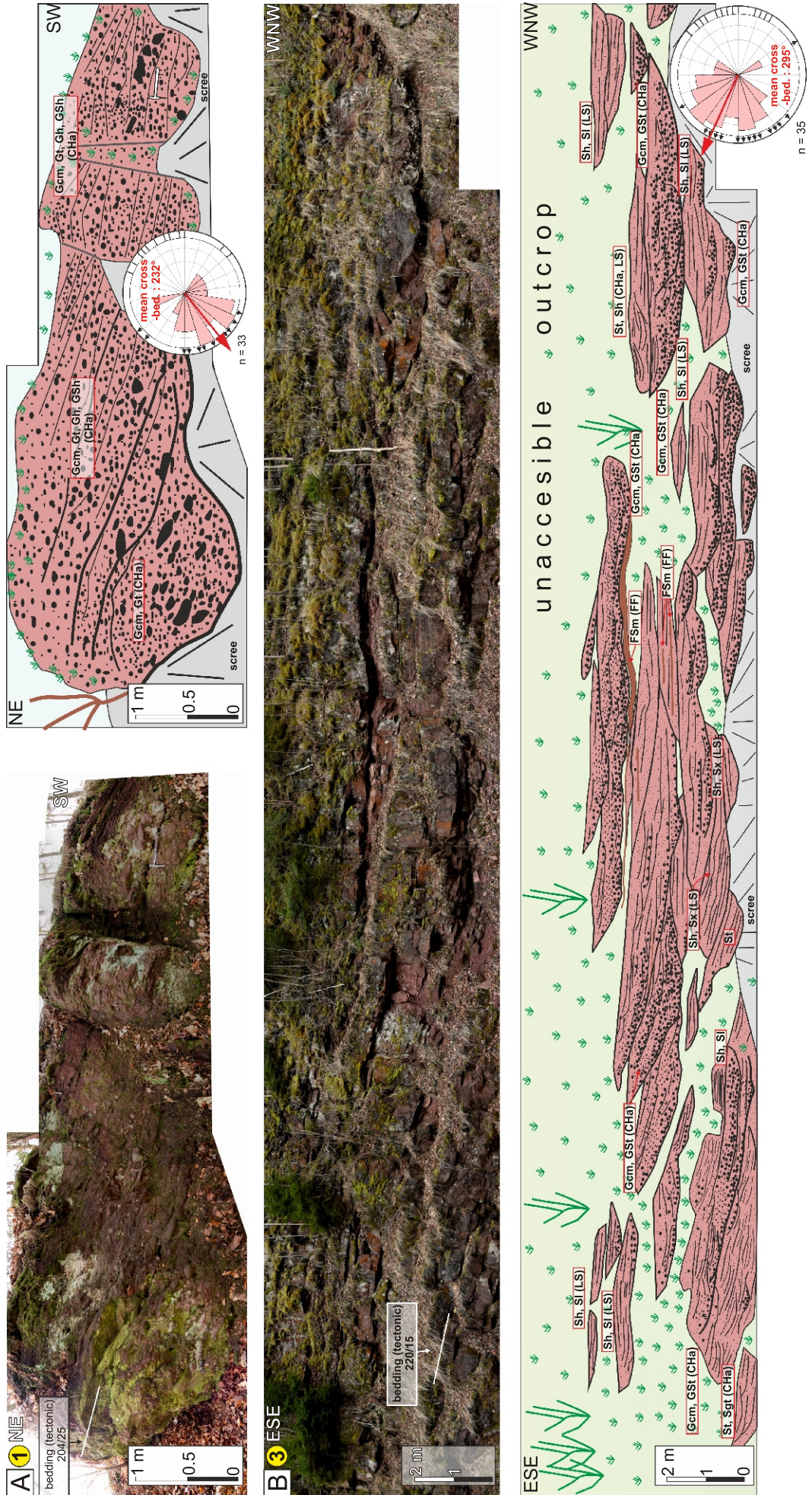


**Fig. 10. Outcrop-scale geometry and main architectural elements of the lowermost Krajanów Formation in the eastern part of the Intra-Sudetic Basin (localities 1, 3)**

The inset rose diagram shows palaeocurrent data: orientation of cross-bedding with mean directions (red arrow) as well as channel axes (black arrows)

plumes, entering the floodplain during waning stages of the flood. Dessication cracks observed on the bedding planes of FSm lithofacies imply drying out of the sediments, probably between flood events (Collinson, 1996). In the study area, the FF architectural element contains also bioturbation features assigned to the *Scoyenia* ichnofacies. This points to stabilisation of the overbank/floodplain areas between major flood events and development of weak pedogenic processes. Fine-grained deposits found within channels record periods of dryness between their rapid infilling.

#### DISCUSSION: FLUVIAL SYSTEM AND PALAEOGEOGRAPHIC DEVELOPMENT OF THE EARLY PERMIAN INTRA-SUDETIC BASIN

Fluvial systems, understood as open, process-response physical systems, are influenced mainly by spatial and temporal changes of climate, base level, tectonics and human impacts (Schumm, 1977; Piégay, 2016). Regional tectonic activity (i.e. fault-controlled subsidence), as well as climate fluctuations, appear to have been the two main, allocyclic controlling factors affecting accommodation space, sediment supply and fluvial architecture in the Carboniferous-Permian Intra-Sudetic Basin (Nemec et al., 1982; Wojewoda and Mastalerz, 1989; Awdankiewicz et al., 2003).

Sedimentological analysis of exposure and selected borehole data (Miecznik, 1989; Fig. 4) shows that the lowermost part of the Krajanów Formation is characterised typically by laterally and vertically amalgamated fluvial channel-fill elements (CHa). Amalgamated channel-fills constitute from 37 to nearly 100% of the deposits within the lowermost portion studied of the Krajanów Formation. The sedimentological characteristics of these deposits (loc. 1) point to a fluvial system dominated by laterally shifting, braided rivers carried a mixed gravel and sand bedload in the form of 3D and 2D dunes, evolving into mid-channel bars (Fig. 11A). Low-angle reactivation surfaces, particularly common in planar cross-strata sets, point to changes in river water stage (Collinson, 1970). Additionally, the occurrence of Gmm lithofacies indicates gravity flows which entered alluvial channels probably during flash floods (Miall, 1996) or formed due to the collapse of river banks (Priddy et al., 2021). The muddy to fine sandy cappings observed within channels in the medial parts of the basin imply channel abandonment and its subsequent drying (Miall, 1996). Overbank deposits are poorly preserved within the lowermost part of the Krajanów Formation due to the high mobility of the channels. The regional climate was arid to semi-arid, with sparse vegetation and limited chemical weathering (Nemec et al., 1982; Wojewoda and Mastalerz, 1989). The riverbanks may have been unstable: this allowed high channel mobility which was limited only by the inherited topography of the basin.

In the upper part of the succession studied, the braided style of fluvial architecture evolved laterally and gradually upwards into non-perennial to ephemeral fluvial strata. Poorly channelized to non-channelized fluvial sheet-like elements (LS) appear to be more abundant in this part of the succession (Fig. 10B). These elements are interpreted as deposits of unconfined sheet flows and/or erosional remnants of wide and shallow channels. The presence of discontinuous intrasets of lithofacies Fm/FSm, also with mudcracks, suggests waning flows and subsequent drying of the sediment surface. Interpreted rapid flood flows in the upper flow regime probably extended laterally beyond the channel margins as sheet floods

and covered large parts of the palaeovalley(s?) in the study area (Fig. 11B). In vertical sections the percentage values of these elements reach 41% (loc. 3).

The gradual change in the fluvial architecture within the Krajanów Formation can be attributed to lateral and temporal changes in the river system rather than to a gradual shift in regional climate (Wojewoda and Mastalerz, 1989). These trends are similar to those observed and described from modern and ancient continental sedimentary basins dominated by terminal fans and, in a broader sense, by distributive fluvial systems (DFSs; Cain and Mountney, 2009; Owen et al., 2015). However, deposits of the lowermost Krajanów Formation display no significant, vertical changes in grain-size distribution (cf. Figs. 6 and 7); this may be explained by a high rate of sediment supply and the occurrence of rapid flood flows in the proximal part of the fluvial system during the early Permian. Downstream decrease in grain size is observed at a larger scale, within the Krajanów Formation understood as a sedimentary megasequence (Miecznik, 1989). The measured palaeocurrent directions indicate that the area drained towards the west, southwest and locally northwest (Fig. 11C). Early Permian (?Asselian) sedimentation in the study area took place within a westwards-sloping alluvial plain, locally followed by ephemeral lake environments in the distal region of the basin (Fig. 11C).

Tectonic activity has been long considered as the main, external control of the sedimentation in the Intra-Sudetic Basin and in other Late Palaeozoic continental basins developed within and around Bohemian Massif (Wojewoda and Mastalerz, 1989; Opluštil et al., 1998). Based on sedimentological study of the Vrchlabí Formation – a time equivalent of the Krajanów Formation in the Krkonoše Piedmont Basin – Schöpfer et al. (2022) postulated that tectonic subsidence played a substantial role during the initial deposition of these deposits. Similarly, the distinct, large-scale cyclic structure of the Permian sedimentary infill of the Intra-Sudetic Basin is attributed to relatively rapid, major tectonic events that resulted in fault-controlled subsidence of the basin floor. The onset of fluvial red bed deposition of the lowermost Krajanów Formation should be also linked with episodic, fault-controlled tectonic activity which led to rejuvenation of relief and, in consequence, an increase in accommodation space in the basin. Simultaneously, uplift of the framing Sowie Mts. Massif, probably along the Gluszyca Fault, led to progradation of an alluvial fan system on the eastern flank of the basin. The sharp contact between the Krajanów Formation and the underlying Lower Anthracosia Shale of the Ludwikowice Formation (cf. Fig. 4) supports the hypothetical notion of relatively rapid uplift of the source area along this tectonically active margin (Don, 1961).

The petrographic composition of the Krajanów Formation is very diverse and points seemingly to multiple source areas within an early Permian sediment routing system. The petrographic characteristic of the Krajanów sandstones – their low textural maturity and a high content of feldspar grains – indicate short-distance transport and the proximity of an uplifted area built chiefly of (weathered?) gneissic or quartz-feldspathic granitic rocks. The occurrence of gneissic detritus within the Krajanów Formation may indicate the Sowie Mts. Massif as the source area for these deposits. Similarly, the petrographic composition of the conglomerate pebbles and the palaeotransport directions obtained from the older, Pennsylvanian deposits and younger, early Permian Słupiec Formation, show that this part of the Intra-Sudetic Basin have been sourced locally from the Sowie Mts. Massif area (Bossowski and Ihnatowicz, 1994; Mastalerz,

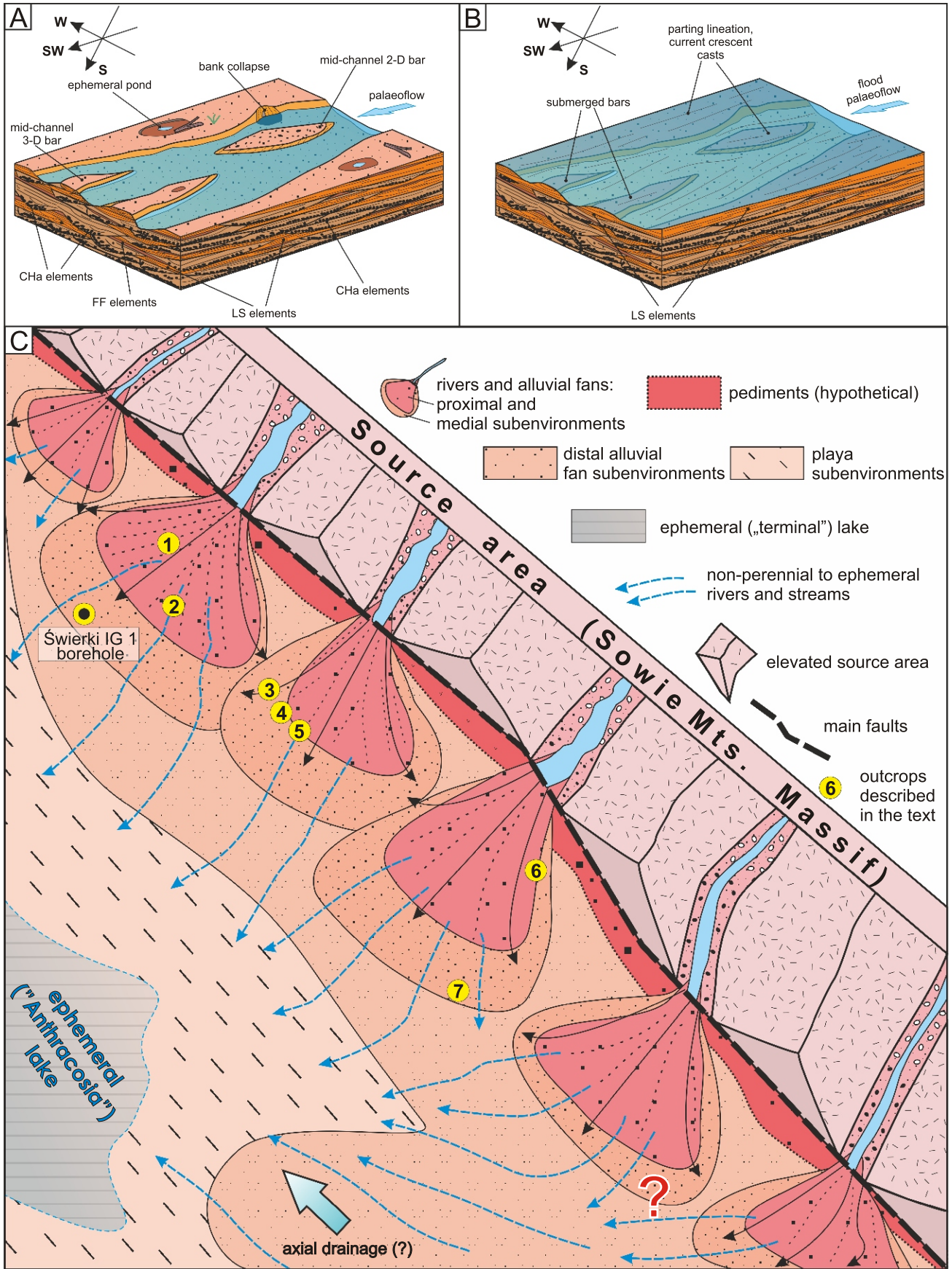


Fig. 11A, B – facies models of the fluvial system of the proximal, eastern part of the Permian Intra-Sudetic Basin during normal (low-stage) flow (A) and during flood flow (B); C – schematic palaeogeographic evolution of the study area in the early Permian (?Asselian, not to scale)

Location of the sections studied and the Świerki IG 1 borehole are marked; for explanations see the text

1996; Kurowski, 2004). Puzzlingly, though, few gneissic pebble-sized clasts derived from this metamorphic unit have been found in the Krajanów Formation (making up c. 3.6%).

The petrography of pebbles in the Permian deposits of the Intra-Sudetic Basin has long been discussed in the literature (Don, 1961; Dzedzic, 1961; Nemeč, 1978; Nemeč et al., 1982). The high degree of roundness of clasts composed of rocks resistant to weathering, such as lydite and quartzite, found in the Krajanów Formation may suggest a distant source area or sediment recycling. These clasts may have been derived from the Silurian and Ordovician rocks exposed currently within the Bardo Structure (e.g., Oberc, 1957; Wajspych, 1978), towards the SE of the study area. As suggested earlier by Oberc and Wójcik (1965), the petrographic composition of the lowermost Krajanów Formation may indicate transport from the Bardzkie and Bystrzyckie Mountains, S and SE of the study area. The derivation of this material from an older, currently unexposed (completely eroded?) massif (hypothetical Southern Massif) sourcing the Intra-Sudetic Basin from the south, should be not excluded (Nemeč, 1978). On the other hand, Dzedzic (1961) inferred that well-rounded pebbles of quartzite and lydite were redeposited from older, Carboniferous (Pennsylvanian) rocks exposed on the eastern flank of the Intra-Sudetic Basin. The high content of the older, reddish-brown sandstones within the deposits studied, as well as clasts of highly cemented quartz conglomerate, points also to an intrabasinal source composed chiefly of Carboniferous strata. Deposits of similar characteristics are typical of the underlying Ludwikowice, Glinik and Żacler formations exposed currently to the east of the study area. Nemeč et al. (1981) also stated that quartzite and lydite pebbles occurring within underlying Carboniferous conglomerates and sandstones constitute "the second-type detritus" which may be derived from "relatively distant source areas". Multiple recycling of clastic material in the Permian Intra-Sudetic Basin was suggested also by Biernacka (2012) and Felicka (2000). Similar petrographic evidence of repeated recycling of fluvial clastic deposits was inferred from petrographic data published by Martínek and Štolfová (2009) from the Krkonoše Piedmont Basin.

On the other hand, the palaeocurrents pattern of the Krajanów Formation in the eastern Intra-Sudetic Basin clearly suggests sediment transport from the east/northeast, i.e. from the Sowie Mts. Massif area. The relatively low content of gneiss pebbles may be explained by limited fluvial incision into the basement rocks and/or partial sedimentary cover of the Sowie Mts. Massif area during the early Permian. The gneissic material derived from this massif, as an upland source area, were carried probably during major flood events to the nearby Intra-Sudetic Basin. This process, combined with the hypothetical axial drainage of the basin towards the NW (cf. Wojewoda and Mastalerz, 1989), may have resulted in the compositional 'dilution' of clastic material in the early Permian Intra-Sudetic Basin. It is concluded that further, detailed petrographic studies and a more systematic approach are needed.

## CONCLUSIONS

The lowermost part of an early Permian Krajanów Formation constitutes a continental fluvial red bed assemblage of coarse-grained strata exposed mainly in the eastern part of the fault-bounded Intra-Sudetic Basin (NE Bohemian Massif). Regional tectonic activity (i.e. fault controlled subsidence) and climate fluctuations appear to have been the two main, allocyclic controlling factors affecting sediment supply and fluvial architecture in this area. During the early Permian (?Asselian) the study area constituted a westwards inclined palaeoslope of the Intra-Sudetic Basin with dominantly westwards and south-westwards fluvial drainage. Towards the west and southwest of the Basin, the coarse-grained sedimentary succession of the Krajanów Formation changes gradually into a coeval fine-grained facies. A fan-like arrangement of palaeocurrent data in the lowermost part of the unit suggests the development of alluvial fans, probably of terminal type, attached to an active fault framing the basin towards the east. Deposition probably occurred in the proximal to medial sub-environments of the fans.

The early Permian (?Asselian) fluvial system in this area was dominated by non-perennial to ephemeral fluvial processes influenced strongly by a semi-arid to arid climate. The fluvial system of the early Permian Intra-Sudetic Basin was fed by episodic flow. Rapid (catastrophic?) flood events led to episodic sedimentation of vertically and laterally amalgamated fluvial channel infills, with abundant upper flow regime structures as well as poorly channelized, laterally extensive sheet-like bodies of sandstone. The overbank deposits are poorly preserved due to frequent lateral shifting of the channels. Soft-sediment deformation structures formed due to river bank collapse events while debris flow facies point to high-energy, waning flows. It is concluded that deposition occurred on broad, terminal-type alluvial fans, probably in their proximal- to medial sub-environments, developed within the distributive fluvial system of the Intra-Sudetic Basin. Petrographic composition and measured palaeocurrent directions show that the sediment was sourced from the framing massifs: the Sowie Mts. Block to the east, the Bardo Structure and a hypothetical Southern Massif to the south/southeast. The study as a whole contributes to understanding of the Permian palaeoenvironment and palaeogeography of the NE part of the Bohemian Massif.

**Acknowledgements.** The research was funded by the Polish National Science Centre (Grant 2017/26/M/ST10/00646). We would like to thank two reviewers: R. Nádaskay (Czech Geological Survey, Prague) and an anonymous reviewer, for their critical reading and many inspiring suggestions which improved the paper. We are grateful to K. Mastalerz for numerous discussions during the preparation of the manuscript.

## REFERENCES

- Allen, J.R.L. (ed.), 1982. Sedimentary structures. Their character and physical basis, I. Developments in Sedimentology, **30A**: 237–270; [https://doi.org/10.1016/S0070-4571\(08\)71000-8](https://doi.org/10.1016/S0070-4571(08)71000-8)
- Al-Masrahy, M.A., Mounney, N.P., 2015. A classification scheme for fluvial-aeolian system interaction in desert-margin settings. *Aeolian Research*, **17**: 67–88; <https://doi.org/10.1016/j.aeolia.2015.01.010>
- Augustyniak, K., Grocholski, A., 1968. Geological structure and outline of the development of the Intra-Sudetic depression. *Biuletyn Instytutu Geologicznego*, **17**: 87–111.
- Awdankiewicz, M., 1999. Volcanism in a late Variscan intramontane trough: Carboniferous and Permian volcanic centres of the Intra-Sudetic Basin, SW Poland. *Geologia Sudetica*, **32**: 13–47.

- Awdankiewicz, M., 2022.** Polyphase Permo-Carboniferous magmatism adjacent to the Intra-Sudetic Fault: constraints from U-Pb SHRIMP zircon study of felsic subvolcanic intrusions in the Intra-Sudetic Basin, SW Poland. *International Journal of Earth Sciences*, **111**: 2199–2224; <https://doi.org/10.1007/s00531-022-02232-y>
- Awdankiewicz, M., Kurowski, L., Mastalerz, K., Raczyński, P., 2003.** The Intra-Sudetic Basin - a record of sedimentary and volcanic processes in late – to post-orogenic tectonic setting. *Geolines*, **16**: 165–183.
- Biernacka, J., 2012.** Detritus from Variscan lower crust in Rotliegend sandstones of the Intra-Sudetic Basin, SW Poland, revealed by detrital high-pyropite garnet. *Annales Societatis Geologorum Poloniae*, **82**: 127–138.
- Billi, P., 2011.** Flash flood sediment transport in a steep sand-bed ephemeral stream. *International Journal of Sediment Research*, **26**: 193–209; [https://doi.org/10.1016/S1001-6279\(11\)60086-3](https://doi.org/10.1016/S1001-6279(11)60086-3)
- Bossowski, A., Ilnatowicz, A., 1994.** Palaeogeography of the uppermost Carboniferous and lowermost Permian deposits in the NE part of the Intra-Sudetic Depression. *Geological Quarterly*, **38** (4): 709–726.
- Bridge, J.S., 2009.** Rivers and Floodplains: Forms, Processes, and Sedimentary Record. John Wiley & Sons, Chichester.
- Bridge, J.S., Best, J.L., 1988.** Flow, sediment transport and bedform dynamics over the transition from dunes to upper-stage plane beds: implications for the formation of planar laminae. *Sedimentology*, **35**: 753–763; <https://doi.org/10.1111/j.1365-3091.1988.tb01249.x>
- Cain, S.A., Mountney, N.P., 2009.** Spatial and temporal evolution of a terminal fluvial fan system: the Permian Organ Rock Formation, South-east Utah, USA. *Sedimentology*, **56**: 1774–1800; <https://doi.org/10.1111/j.1365-3091.2009.01057.x>
- Camarasa-Belmonte, A.M., 2016.** Flash floods in Mediterranean ephemeral streams in Valencia Region (Spain). *Journal of Hydrology*, **541**: 99–115; <https://doi.org/10.1016/j.jhydrol.2016.03.019>
- Cartigny, M.J.B., Ventra, D., Postma, G., van Den Berg, J.H., 2014.** Morphodynamics and sedimentary structures of bedforms under supercritical-flow conditions: New insights from flume experiments. *Sedimentology*, **61**: 712–748; <https://doi.org/10.1111/sed.12076>
- Collinson, J.D., 1970.** Bedforms of the Tana river, Norway. *Geografiska Annaler: Series A, Physical Geography*, **52**: 31–56.
- Collinson, J.D., 1996.** Alluvial sediments. In: *Sedimentary Environments: Processes, Facies and Stratigraphy*: 37–82. Blackwell Publishing.
- Colombera, L., Mountney, N.P., McCaffrey, W.D., 2013.** A quantitative approach to fluvial facies models: Methods and example results. *Sedimentology*, **60**: 1526–1558; <https://doi.org/10.1111/sed.12050>
- Coward, M., 1995.** Structural and tectonic setting of the Permo-Triassic basins of northwest Europe. *Geological Society Special Publications*, **91**: 7–39; <https://doi.org/10.1144/gsl.sp.1995.091.01.02>
- Cymerman, Z., Badura, J., Ilnatowicz, A., 2015a.** Szczegółowa mapa geologiczna Polski 1:50 000, arkusz 868, Nowa Ruda (in Polish). Państwowy Instytut Geologiczny – Państwowy Instytut Badawczy, Warszawa.
- Cymerman, Z., Badura, J., Ilnatowicz, A., 2015b.** Objasnienia do Szczegółowej mapy geologicznej Polski w skali 1:50 000, arkusz (868), Nowa Ruda (in Polish). Państwowy Instytut Geologiczny – Państwowy Instytut Badawczy, Warszawa.
- Dathe, E., 1904a.** Geologische Karte von Preußen und benachbarten Bundesstaaten 1:25 000. Blatt Rudolfswaldau. Lieferung 115. Königlich Preußischen Geologischen Landesanstalt, Berlin.
- Dathe, E., 1904b.** Geologische Karte von Preußen und benachbarten Bundesstaaten 1:25 000. Blatt Neurode. Lieferung 115. Königlich Preußischen Geologischen Landesanstalt und Bergakademie, Berlin.
- Deluca, J.L., Eriksson, K.A., 1989.** Controls on synchronous ephemeral- and perennial-river sedimentation in the middle sandstone member of the Triassic Chinle Formation, northeastern New Mexico, U.S.A. *Sedimentary Geology*, **61**: 155–175; [https://doi.org/10.1016/0037-0738\(89\)90056-0](https://doi.org/10.1016/0037-0738(89)90056-0)
- Don, J., 1961.** The Permo-Carboniferous of the Nowa Ruda region (in Polish with English summary). *Zeszyty Naukowe Uniwersytetu Wrocławskiego. Nauki Przyrodnicze. Nauka o Ziemi*, **3**: 3–54.
- Doornbal, J.C., Stevenson, A.G. (ed.), 2010.** Petroleum Geological Atlas of the Southern Permian Basin Area. EAGE Publications b.v. (Houten).
- Dziedzic, K., 1959.** Comparison of Rotliegendes sediments in the region of Nowa Ruda and Świerzawa (in Polish with English summary). *Kwartalnik Geologiczny*, **3** (4): 831–846.
- Dziedzic, K., 1961.** Lower Permian in the Intrasudetic Basin (in Polish with English summary). *Studia Geologica Polonica*, **6**: 1–124.
- Dziedzic, K., Teisseyre, A.K., 1990.** The Hercynian molasse and younger deposits in the Intra-Sudetic Depression, SW Poland. *Neues Jahrbuch für Geologie und Paläontologie*, **179**: 285–305.
- Felicka, E., 2000.** Heavy minerals in the Carboniferous sediments of the Intra-Sudetic Basin as palaeogeographic indicators. *Geologia Sudetica*, **33**: 49–65.
- Foley, M.G., 1978.** Scour and fill in steep, sand-bed ephemeral streams. *GSA Bulletin*, **89**: 559–570; [https://doi.org/10.1130/0016-7606\(1978\)89<559:SAFISS>2.0.CO;2](https://doi.org/10.1130/0016-7606(1978)89<559:SAFISS>2.0.CO;2)
- Gawroński, O., 1959.** Szczegółowa mapa geologiczna Sudetów w skali 1:25 000, arkusz Jugów. Instytut Geologiczny, Warszawa.
- Glennie, K.W., 1970.** Desert sedimentary environments. *Developments in Sedimentology*, **14**.
- Głuszyński, A., Aleksandrowski, P., 2022.** Late Cretaceous-Early Palaeogene inversion-related tectonic structures at the NE margin of the Bohemian Massif (SW Poland and northern Czechia). *Solid Earth*, **13**: 1219–1242; <https://doi.org/10.5194/se-13-1219-2022>
- Górecka, T., 1981.** Results of palynological studies of the Youngest Carboniferous of the Lower Silesia (in Polish with English summary). *Prace Naukowe Instytutu Górnictwa Politechniki Wrocławskiej, Monografie*, **19**: 1–58.
- Górecka-Nowak, A., 1995.** Palynostratigraphy of the Westphalian deposits of the north-western part of the Intrasudetic Basin (in Polish with English summary). *Acta Universitatis Wratislaviensis, Prace Geologiczno-Mineralogiczne*, **40**.
- Górecka-Nowak, A., Jankowska, A., Muszer, J., 2021.** Age revision of Carboniferous rocks in the northern part of the Intra-Sudetic Basin (SW Poland) based on microspore data. *Geological Quarterly*, **65**: 8; <http://dx.doi.org/10.7306/gq.1581>
- Harms, J.C., Southard, J.B., Spearing, D.R., Walker, R.G., 1975.** Depositional environments as interpreted from primary sedimentary structures and stratification sequences. *SEPM Short Course Notes*, **2**; <https://doi.org/10.2110/scn.75.02>
- Hein, F.J., Walker, R.G., 1977.** Bar evolution and development of stratification in the gravelly, braided, Kicking Horse River, British Columbia. *Canadian Journal of Earth Sciences*, **14**: 562–570. <https://doi.org/10.1139/e77-058>
- Holub, V., 1972.** Permian of the Bohemian Massif. *International Sedimentary Petrographical Series*, **15**: 137–188.
- Holub, V., 1975.** Permian basins in the Bohemian Massif. *NATO Advanced Study Institute Series*, **22**: 57.
- Horn, B.L.D., Goldberg, K., Schultz, C.L., 2018.** Interpretation of massive sandstones in ephemeral fluvial settings: a case study from the Upper Candelária Sequence (Upper Triassic, Paraná Basin, Brazil). *Journal of South American Earth Sciences*, **81**: 108–121; <https://doi.org/10.1016/j.jsames.2017.10.009>
- Ilnatowicz, A., 2005.** Depositional conditions of the Glinik Formation (Intra-Sudetic Basin) (in Polish with English summary). *Biuletyn Państwowego Instytutu Geologicznego*, **415**: 101–151.
- Ilnatowicz, A., Cymerman, Z., Awdankiewicz, H., Ciszek, D., 2017a.** Szczegółowa mapa geologiczna Polski 1:50 000. Arkusz 867, Radków (in Polish). Państwowy Instytut Geologiczny – Państwowy Instytut Badawczy, Warszawa.
- Ilnatowicz, A., Cymerman, Z., Awdankiewicz, H., Ciszek, D., Badura, J., 2017b.** Objasnienia do Szczegółowej mapy geologicznej Polski w skali 1:50 000. Arkusz Radków (867) (in Polish). Państwowy Instytut Geologiczny – Państwowy Instytut Badawczy, Warszawa.
- Jerzykiewicz, J., 1987.** Latest Carboniferous (Stephanian) and Early Permian (Autunian) palynological assemblages from the Intrasudetic Basin, Southwestern Poland. *Palynology*, **11**: 117–131.

- Karcz, I., 1972.** Sedimentary structures formed by flash floods in southern Israel. *Sedimentary Geology*, **7**: 161–182; [https://doi.org/10.1016/0037-0738\(72\)90001-2](https://doi.org/10.1016/0037-0738(72)90001-2)
- Karnkowski, P.H., 1999.** Origin and evolution of the Polish Rotliegend Basin. *Polish Geological Institute Special Papers*, **3**: 1–93.
- Kelly, S.B., Olsen, H., 1993.** Terminal fans - a review with reference to Devonian examples. *Sedimentary Geology*, **85**: 339–374; [https://doi.org/10.1016/0037-0738\(93\)90092-J](https://doi.org/10.1016/0037-0738(93)90092-J)
- Kędzior, A., Popa, M.E., 2018.** An early Jurassic braided river system from Mehadia, south Carpathians, Romania. *Geological Quarterly*, **62** (2): 415–432; <https://doi.org/10.7306/gq.1415>
- Kiersnowski, H., 1997.** Depositional development of the Polish Upper Rotliegend Basin and evolution of its sediment source areas. *Geological Quarterly*, **41** (4): 433–456.
- Kiersnowski, H., 2013.** Late Permian aeolian sand seas from the Polish Upper Rotliegend basin in the context of palaeoclimatic periodicity. *Geological Society Special Publications*, **376**: 431–456; <https://doi.org/10.1144/sp376.20>
- Kiersnowski, H., Buniak, A., 2016.** Sand sheets interaction with aeolian dune, alluvial and marginal playa beds in Late Permian Upper Rotliegend setting (western part of the Poznań Basin, Poland). *Geological Quarterly*, **60** (4): 771–800; <http://doi.org/10.7306/gq.1336>
- Kiersnowski, H., Peryt, T., 2023.** Baseny permskie (in Polish with English summary). *Prace Państwowego Instytutu Geologicznego*, **207**: 49–62.
- Kiersnowski, H., Kowalski, A., Ploch, I., Raczyński, P., 2021.** Early Permian ichnofossils assemblage from Bieganów quarry and surrounding localities, Słupiec Fm. – Intrasudetic Basin. *Book of Abstracts: 235. 35th Meeting of Sedimentology, Prague, Czech Republic*.
- Kowalski, A., 2020.** Triassic palaeogeography of NE Bohemian Massif based on sedimentological record in the Wleń Graben and the Krzeszów Brachysyncline (SW Poland). *Annales Societatis Geologorum Poloniae*, **90**: 125–148; <https://doi.org/10.14241/asgp.2020.09>
- Kowalski, A., 2021.** Late Cretaceous palaeogeography of NE Bohemian Massif: diachronous sedimentary successions in the Wleń Graben and Krzeszów Brachysyncline (SW Poland). *Annales Societatis Geologorum Poloniae*, **91**: 1–36; <https://doi.org/10.14241/asgp.2021.05>
- Krechowicz, J., 1964.** Szczegółowa mapa geologiczna Sudetów w skali 1:25 000, arkusz Radków (in Polish). *Instytut Geologiczny, Warszawa*.
- Krechowicz, J., 1965.** Objaśnienia do Szczegółowej mapy geologicznej Sudetów w skali 1:25 000, arkusz Radków (in Polish). *Wyd. Geol., Warszawa*.
- Krechowicz, J., Berezowska, B., 1968.** Objaśnienia do Szczegółowej mapy geologicznej Sudetów w skali 1:25 000, arkusz Ludwikowice Kłodzkie (in Polish). *Wyd. Geol., Warszawa*.
- Krechowicz, J., Kisieliwski, F., 1965.** Szczegółowa Mapa geologiczna Sudetów w skali 1:25 000, arkusz Ludwikowice Kłodzkie (in Polish). *Instytut Geologiczny, Warszawa*.
- Kurowski, L., 1993.** Punkt. 8. Ludwikowice Kłodzkie. In: *II Krajowe Spotkanie Sedymetologów. Baseny sedymentacyjne. Procesy, osady, architektura. Przewodnik. Wycieczki, referaty, postery: 88–89.* Instytut Nauk Geologicznych Uniwersytetu Wrocławskiego, Wrocław.
- Kurowski, L., 1995.** Stop 13. Ludwikowice Kłodzkie, old quarry west of the village. In: *XIII International Congress on Carboniferous-Permian (XIII ICC-P). August 28–September 2, 1995. Guide to Excursion B1. Sedimentary record of the Variscan orogeny and climate – Intra-Sudetic Basin, Poland and Czech Republic: 31–33.* Polish Geological Institute, Kraków, Poland.
- Kurowski, L., 1998.** Fluvial sedimentology of the Biały Kamień Formation (Upper Carboniferous, Sudetes, Poland). *Geologia Sudetica*, **31**: 69–77.
- Kurowski, L., 2004.** Fluvial sedimentation of sandy deposits of the Słupiec Formation (Middle Rotliegendes) near Nowa Ruda (Intra-Sudetic Basin, SW Poland). *Geologia Sudetica*, **36**: 21–38.
- Lange, J., 2005.** Dynamics of transmission losses in a large arid stream channel. *Journal of Hydrology*, **306**: 112–126; <https://doi.org/10.1016/j.jhydrol.2004.09.016>
- Leclair, S.F., Bridge, J.S., 2001.** Quantitative interpretation of sedimentary structures formed by river dunes. *Journal of Sedimentary Research*, **71**: 713–716; <https://doi.org/10.1306/2DC40962-0E47-11D7-8643000102C1865D>
- Long, D.G.F., 2006.** Architecture of pre-vegetation sandy-braided perennial and ephemeral river deposits in the Palaeoproterozoic Athabasca Group, northern Saskatchewan, Canada as indicators of Precambrian fluvial style. *Sedimentary Geology*, **190**: 7–95; <https://doi.org/10.1016/j.sedgeo.2006.05.006>
- Lorenc, S., 1993.** Distribution, lithology and approximate geochemical features of the Sudetes black shales. *Prace Geologiczno-Mineralogiczne*, **33**: 179–208.
- Lowe, D.G., Arnott, R.W.C., 2016.** Composition and architecture of braided and sheetflood-dominated ephemeral fluvial strata In the Cambrian-Ordovician Potsdam Group: a case example of the morphodynamics of Early Phanerozoic fluvial systems and climate change. *Journal of Sedimentary Research*, **86**: 587–612; <https://doi.org/10.2110/jsr.2016.39>
- Lützner, H., 1988.** Sedimentology and Basin Development of Intramontane Rotliegend Basins in Central-Europe. *Zeitschrift für Geologische Wissenschaften*, **16**: 845–863.
- Malkovský, M., 1987.** The Mesozoic and Tertiary basins of the Bohemian Massif and their evolution. *Tectonophysics*, **137**: 31–42; [https://doi.org/10.1016/0040-1951\(87\)90311-8](https://doi.org/10.1016/0040-1951(87)90311-8)
- Martínek, K., Štolfová, K., 2009.** Provenance study of Permian non-marine sandstones and conglomerates of the Krkonoše Piedmont Basin (Czech Republic): exotic marine limestone pebbles, heavy minerals and garnet composition. *Bulletin of Geosciences*, **84**: 555–568.
- Mastalerz, K., 1995.** Deposits of high-density turbidity currents on fan-delta slopes: an example from the upper Visean Szczawno formation, Intrasudetic Basin, Poland. *Sedimentary Geology*, **98**: 121–146; [https://doi.org/10.1016/0037-0738\(95\)00030-C](https://doi.org/10.1016/0037-0738(95)00030-C)
- Mastalerz, K., 1996.** Fluvial sedimentation of the coal-bearing Żacler Formation (Westphalian) in the Wałbrzych Basin, SW Poland (in Polish with English summary). *Acta Universitatis Wratislaviensis. Prace Geologiczno-Mineralogiczne*, **52**: 21–85.
- Mastalerz, K., Nehyba, S., 1997.** Comparison of Rotliegende lacustrine depositional sequences from the Intrasudetic, North-Sudetic and Boskovice basins (Central Europe). *Geologia Sudetica*, **30**: 21–57.
- Mastalerz, K., Kurowski, L., Wojewoda, J., 1993.** Litostratygrafia i ewolucja basenu śródsudeckiego w karbonie i permie (in Polish). *II Krajowe Spotkanie Sedymetologów. Baseny sedymentacyjne – procesy, osady, architektura.* Wrocław, Sudety, 4–7 września: 65–73. *Instytut Nauk Geologicznych Uniwersytetu Wrocławskiego, Wrocław*.
- Miall, A.D., 1977.** A review of the braided-river depositional environment. *Earth-Science Reviews*, **13**: 1–62; [https://doi.org/10.1016/0012-8252\(77\)90055-1](https://doi.org/10.1016/0012-8252(77)90055-1)
- Miall, A.D., 1996.** *The Geology of Fluvial Deposits. Sedimentary Facies, Basin Analysis, and Petroleum Geology.* Springer.
- Miall, A., 2014.** *Fluvial Depositional Systems.* Springer International Publishing.
- Miecznik, J.B., 1989.** The Upper Silesian and Lower Autunian from NE limb of the Intra-Sudetic Depression (in Polish with English summary). *Biuletyn Państwowego Instytutu Geologicznego*, **363**: 5–39.
- Mroczkowski, J., Mader, D., 1985.** Sandy inland braidplain deposition with local aeolian sedimentation in the lower and middle parts of the Buntsandstein and sandy coastal braidplain deposition in the topmost Zechstein in the Sudetes (Lower Silesia, Poland). *Lecture Notes in Earth Sciences*, **4**: 165–195.
- Nemec, W., 1978.** Tectonically controlled alluvial sedimentation in the Słupiec Formation (Lower Permian) of Intrasudetic Basin. In: *International Symposium Central European Permian. Jablonna, April 27–29, 1978: 294–311.*
- Nemec, W., 1984.** Wałbrzych Beds (Lower Namurian, Wałbrzych Coal Measures): analysis of alluvial sedimentation in a coal basin (in Polish with English summary). *Geologia Sudetica*, **19**: 7–73.
- Nemec, W., Porębski, S.J., Teisseyre, A.K., 1982.** Explanatory notes to the lithotectonic molasse profile of the Intra-Sudetic Basin, Polish part (Sudety Mts., Carboniferous-Permian). *Veröffentlichungen des Zentralinstituts für Physik der Erde*, **66**: 267–278.
- North, C.P., Taylor, K.S., 1996.** Ephemeral-fluvial deposits: Integrated outcrop and simulation studies reveal complexity. *AAPG Bulletin*, **80**: 811–830; <https://doi.org/10.1306/64ED88D6-1724-11D7-8645000102C1865D>
- Nowak, G.J., 1998.** Microscopic identification and classification of organic matter of the Upper Carboniferous Anthracosia Shales, Intra-Sudetic Depression, southwestern Poland. *Geological Quarterly*, **42** (1): 41–58.

- Nowak, G.J., 2007.** Comparative studies of organic matter petrography of the late Palaeozoic black shales from Southwestern Poland. *International Journal of Coal Geology*, **71**: 568–585; <https://doi.org/10.1016/j.coal.2007.01.004>
- Nowak, G., Górecka-Nowak, A., Karcz, P., 2022.** Petrographic, palynological and geochemical recognition of dispersed organic matter in the black Anthracosia Shales (Sudetes, south-west Poland). *Geological Quarterly*, **66** (1): 36; <https://doi.org/10.7306/gq.1668>
- Oberc, J., 1957.** Region Gór Bardzkich (Sudety). Wyd. Geol., Warszawa.
- Oberc, J., 1972.** Sudety i obszary przyległe (in Polish). Budowa Geologiczna Polski. Vol. 4. Tektonika, Part 2. Wyd. Geol., Warszawa.
- Oberc, J., Wójcik, L., 1965.** Objaśnienia do Szczegółowej mapy geologicznej Sudetów. Arkusz Nowa Ruda 1:25 000 (in Polish). Wyd. Geol., Warszawa.
- Olsen, H., 1987.** Ancient ephemeral stream deposits: a local terminal fan model from the Bunter Sandstone Formation (L. Triassic) in the Tønder-3, -4 and -5 wells, Denmark. *Geological Society Special Publications*, **35**: 69–86; <https://doi.org/10.1144/GSL.SP.1987.035.01.06>
- Opluštil, S., Pešek, J., 1998.** Stratigraphy, palaeoclimatology and palaeogeography of the Late Palaeozoic continental deposits in the Czech Republic. *Geodiversitas*, **20**: 597–620.
- Opluštil, S., Schmitz, M., Kachlík, V., Štamberg, S., 2016.** Re-assessment of lithostratigraphy, biostratigraphy, and volcanic activity of the Late Palaeozoic Intra-Sudetic, Krkonoše-Piedmont and Mnichovo Hradiště basins (Czech Republic) based on new U-Pb CA-ID-TIMS ages. *Bulletin of Geosciences*, **91**: 399–432; <https://doi.org/10.3140/bull.geosci.1603>
- Owen, A., Nichols, G.J., Hartley, A.J., Weissmann, G.S., Scuderi, L.A., 2015.** Quantification of a distributive fluvial system: The Salt Wash DFS of the Morrison Formation, SW U.S.A. *Journal of Sedimentary Research*, **85**: 544–561; <https://doi.org/10.2110/jsr.2015.35>
- Picard, M.D., High, L.R.Jr., 1973.** Sedimentary Structures of Ephemeral Streams. *Developments in Sedimentology*, **17**.
- Piégay, H., 2016.** System approaches in fluvial geomorphology. In: *Tools in Fluvial Geomorphology* (eds. G.M. Kondolf and H. Piégay): 77–102. John Wiley & Sons; <https://doi.org/10.1002/9781118648551.ch5>
- Pokorski, J., 1998.** Plate 3, Late Rotliegend, Noteć Sub-group palaeogeography. In: *Palaeogeographical atlas of the epicontinental Permian and Mesozoic in Poland* (eds. R. Dadlez, S. Marek and J. Pokorski). Państwowy Instytut Geologiczny, Warszawa.
- Priddy, C.L., Clarke, S.M., 2020.** The sedimentology of an ephemeral fluvial-aeolian succession. *Sedimentology*, **67**: 2392–2425; <https://doi.org/10.1111/sed.12706>
- Priddy, C.L., Clarke, S.M., 2021.** Spatial variation in the sedimentary architecture of a dryland fluvial system. *Sedimentology*, **68**: 2887–2917; <https://doi.org/10.1111/sed.12876>
- Priddy, C.L., Regis, A.V., Clarke, S.M., Leslie, A.G., Dodd, T.J.H., 2021.** localized bank collapse or regional event? – a study of distinct contorted heterolithic facies observed in the Lower Jurassic Kayenta Formation, Utah and Arizona. *Geology of the Intermountain West*, **8**: 27–44; <https://doi.org/10.31711/giw.v8.pp27-44>
- Reid, I., Frostick, L.E., 1987.** Flow dynamics and suspended sediment properties in arid zone flash floods. *Hydrological Processes*, **1**: 239–253; <https://doi.org/10.1002/hyp.3360010303>
- Rust, B.R., 1972.** Structure and process in a braided river. *Sedimentology*, **18**: 221–245; <https://doi.org/10.1111/j.1365-3091.1972.tb00013.x>
- Sawicki, L., 1995.** Geological Map of Lower Silesia with Adjacent Czech and German Territories (without Quaternary deposits). Państwowy Instytut Geologiczny, Warszawa.
- Schöpfer, K., Nádaskay, R., Martinek, K., 2022.** Evaluation of climatic and tectonic imprints in fluvial successions of an Early Permian depositional system (Asselian Vrchlabí Formation, Krkonoše Piedmont Basin, Czech Republic). *Journal of Sedimentary Research*, **92**: 275–303; <https://doi.org/10.2110/jsr.2020.137>
- Schumm, S.A., 1977.** *The Fluvial System*. John Wiley & Sons.
- Scotese, C.R., 2013.** Earliest Permian Globe (Earliest Permian\_Pgeog\_344.kmz, Google Earth format), [www.globalgeology.com](http://www.globalgeology.com), PALAEOMAP Project, Evanston, IL; <http://dx.doi.org/10.13140/2.1.4674.3689>
- Shanfield, M., Bourke, S.A., Zimmer, M.A., Costigan, K.H., 2021.** An overview of the hydrology of non-perennial rivers and streams. *WIREs Water*, **8**: e1504; <https://doi.org/10.1002/wat2.1504>
- Stear, W.M., 1985.** Comparison of the bedform distribution and dynamics of modern and ancient sandy ephemeral flood deposits in the southwestern Karoo region, South Africa. *Sedimentary Geology*, **45**: 209–230; [https://doi.org/10.1016/0037-0738\(85\)90003-X](https://doi.org/10.1016/0037-0738(85)90003-X)
- Teisseyre, A.K., 1975.** Sedimentology and palaeogeography of the Kulm alluvial fans in the western Intrasudetic Basin (Central Sudetes, SW Poland) (in Polish with English summary). *Geologia Sudetica*, **9**: 7–89.
- Teisseyre, A.K., 1991.** River classification in the light of analysis of the fluvial system and hydraulic geometry (in Polish with English summary). *Prace Geologiczno-Mineralogiczne*, **22**: 1–210.
- Tooth, S., 2000.** Process, form and change in dryland rivers: a review of recent research. *Earth-Science Reviews*, **51**: 67–107; [https://doi.org/10.1016/S0012-8252\(00\)00014-3](https://doi.org/10.1016/S0012-8252(00)00014-3)
- Tunbridge, I.P., 1984.** Facies model for a sandy ephemeral stream and clay playa complex; the Middle Devonian Trentishoe Formation of North Devon, U.K. *Sedimentology*, **31**: 697–715; <https://doi.org/10.1111/j.1365-3091.1984.tb01231.x>
- Turnau, E., Żelaźniewicz, A., Franke, W., 2002.** Middle to early late Viséan onset of late orogenic sedimentation in the Intra-Sudetic Basin, West Sudetes: miospore evidence and tectonic implication. *Geologia Sudetica*, **34**: 9–16.
- Uličný, D., Martinek, K., Grygar, R., 2002.** Syndepositional geometry and post-depositional deformation of the Krkonoše Piedmont Basin: a preliminary model. *Geolines*, **14**: 101–102.
- Wajsprych, B., 1978.** Allochthonous Palaeozoic rocks in the Viséan of the Bardzkie Mts. (Sudetes) (in Polish with English summary). *Annales Societatis Geologorum Poloniae*, **48**: 99–127.
- Weissmann, G.S., Hartley, A.J., Nichols, G.J., Scuderi, L.A., Olson, M., Buehler, H., Banteah, R., 2010.** Fluvial form in modern continental sedimentary basins: Distributive fluvial systems. *Geology*, **38**: 39–42; <https://doi.org/10.1130/G30242.1>
- Williams, G.E., 1971.** Flood deposits of the sand-bed ephemeral streams of central Australia. *Sedimentology*, **17**: 1–40; <https://doi.org/10.1111/j.1365-3091.1971.tb01128.x>
- Wojewoda, J., 1997.** Upper Cretaceous littoral-to-shelf succession in the Intrasudetic Basin and Nysa Trough, Sudety Mts. *Obszary ródłowe: Zapis w Osadach*, **1**: 81–96.
- Wojewoda, J., Mastalerz, K., 1989.** Climate evolution, allo- and autocyclic sedimentation: an example from the Permo-Carboniferous continental deposits of the Sudetes, SW Poland (in Polish with English summary). *Przegląd Geologiczny*, **432**: 173–180.
- Wojewoda, J., Rauch, M., Kowalski, A., 2016.** Synsedimentary seismotectonic features in Triassic and Cretaceous sediments of the Intrasudetic Basin (U Devěti křížů locality) – regional implications. *Geological Quarterly*, **60** (2): 355–364; <https://doi.org/10.7306/gq.1279>
- Wójcik, L., 1958.** Szczegółowa mapa geologiczna Sudetów w skali 1:25 000, arkusz Nowa Ruda (in Polish). Instytut Geologiczny, Warszawa.
- Wójcik-Taboń, P., Dąbek, J., Nowak, G., 2021.** Preliminary mineralogical characteristics of the Anthracosia Shales from the Intra-Sudetic Synclinorium (in Polish with English summary). *Przegląd Geologiczny*, **69**: 389–392; <https://doi.org/10.7306/2021.23>
- Żakowa, H., 1958.** Upper Viséan of the Lower Carboniferous Intrasudetic Basin (in Polish with English summary). *Geological Quarterly*, **2** (3): 609–625.
- Żelaźniewicz, A., Aleksandrowski, P., 2008.** Tectonic subdivision of Poland: southwestern Poland (in Polish with English summary). *Przegląd Geologiczny*, **56**: 904–911.
- Żelaźniewicz, A., Aleksandrowski, P., Buła, Z., Karnkowski, P.H., Konon, A., Oszczypko, N., Ślącza, A., Żaba, J., Żyto, K., 2011.** Tectonic subdivision of Poland (in Polish). *Komitet Nauk Geologicznych PAN, Wrocław*.